UC-25

BDX-613-512

STRESS-CRACKING AND FRACTURE TOUGHNESS OF POLYCARBONATE MATERIAL

F. W. LaMar, Project Leader

Published July, 1971

Prepared for the
United States Atomic Energy Commission
Under Contract Number AT(29-1)-613 USAEC

Bendix Kansas City Division

DISCLAIMER

UC-25

STRESS-CRACKING AND FRACTURE TOUGHNESS OF POLYCARBONATE MATERIAL

BDX-613-512

July, 1971

Prepared by:
F. W. LaMar
Department 421

Technical Communications

Bendix Kansas City Division

THIS PAGE

WAS INTENTIONALLY

LEFT BLANK

THE BENDIX CORPORATION
KANSAS CITY DIVISION
KANSAS CITY, MISSOURI
A prime contractor for the Atomic Energy Commission
Contract Number AT(29-1)-613 USAEC

THIS PAGE

WAS INTENTIONALLY

LEFT BLANK

ABSTRACT

Stress-cracks in polycarbonate material have proven detrimental to the service life of polycarbonate parts. Specimens dead-loaded in tension and exposed to normal and humid atmospheres developed large, numerous stress-cracks and are expected to fail. It was found that stress-cracks shorten fatigue life and occur readily at stress levels well below polycarbonate yield strength in tensile creep, fatigue, and multiaxial tension tests.

THIS PAGE

WAS INTENTIONALLY

LEFT BLANK

CONTENTS

THIS PAGE

WAS INTENTIONALLY

LEFT BLANK

ILLUSTRATIONS

THIS PAGE

WAS INTENTIONALLY

LEFT BLANK

THIS PAGE

WAS INTENTIONALLY

LEFT BLANK

TABLES

THIS PAGE

WAS INTENTIONALLY

LEFT BLANK

SUMMARY

This project was undertaken to determine the effect of stress-cracking on the life of polycarbonate parts. Specific objectives were to characterize polycarbonate materials, to study stress-cracking in polycarbonates, and to establish, if possible, predictor-variables for significant stress-cracks.

The first series of tests indicated that polycarbonate was susceptible to stress-cracking when exposed to multiaxial tension, creep, and low plastic strain. Since these tests were influenced by residual processing stresses, attempts were made to reduce residual stresses and to determine the size at which stress-cracks become critical (the point at which a sharp crack propagates to failure in a cataclysmic manner), propagate suddenly, and cause material failure. A second test series was then run. The mechanisms which cause uniaxial tensile failure and stress-crack propagation were determined, as was the elastic limit for injection-molded material. Annealing studies for removal of residual stresses were continued. A two-by-two factorial experiment performed in an argon atmosphere showed that most residual stresses can be relieved by exposure to 320°F for 100 hours. Yield strength was increased, and, although ductility decreased somewhat and specimens shrank, discoloration during annealing in air was eliminated. A separate project on residual stress effects has been initiated.

Experiments using fracture toughness theories for determining the significance of stress-cracks in polycarbonate were carried out. Crack lengths were predicted to be critical if more than 0.156 inch in length, which is an order of magnitude lower than expected. Since critical crack lengths vary considerably with processing and specimen geometry, three more series of tests were conducted and specimen geometry was varied. The plastic zone size and shape at the tip of propagating cracks, (the plastic compliance factor) was measured. The resulting photoelastic fringes were so numerous that the elastic-plastic boundary could not be determined. The data, however, allowed theoretical calculations which showed that the plastic compliance factor increased the predicted crack length only 12 percent. Some specimens in this test series failed at a net section stress below the elastic limit. Finally, the notch sensitivity ratio was calculated and showed that stress-cracking in polycarbonates probably will result in failures in some service parts.

As a result of these activities, it is concluded that:

- Polycarbonate material stress-cracks readily at stress levels well below its yield strength in tensile creep, uniaxial fatigue, and biaxial tension;
- High humidity increases susceptibility to stress-cracking;

- Notch sensitivity ratios indicate that small stress-cracks may cause failure in polycarbonate parts in service;

- Fracture toughness tests indicate that cracks as small as 0.021 inch long may cause failure of parts in service;

- Residual stresses can be practically eliminated by a high temperature anneal at some expense to ductility;

- Fracture toughness appears to be an effective criterion for predicting significant stress-crack sizes;

- Stress-cracks greatly reduce the endurance limit of polycarbonate;

- Stress-cracks in polycarbonate are greatly influenced by processing methods and the design factors of geometry and deflection; and

- The ductility of polycarbonate appears to prevent stress-cracking in uniaxial tensile tests and impact tests.

As a result of these studies of polycarbonate stress-cracking, it is recommended that:

- The dead-load creep tests be continued, and additional specimens be tested, because it is believed that stress-cracks in present specimens will eventually cause failure;

- Fracture toughness tests be continued using thicker and wider specimens because stress-cracking is more severe under these conditions; and

- Effects of stress-cracking on low cycle plastic strain be investigated because many service parts will undergo this type of loading.

DISCUSSION

SCOPE AND PURPOSE

Stress-cracking in polycarbonates was investigated to determine if such cracks are detrimental to the service life of polycarbonate parts. The investigation was conducted to characterize polycarbonates, to observe stress-cracking and subsequent effects on polycarbonate materials, and to determine what variables, if any, will predict significant stress-cracking in polycarbonate materials.

PRIOR WORK

Originally the Bendix Test Laboratory was asked by the Materials Engineering Department to run a three-phase test on Lexan polycarbonate to determine if it was significantly affected by stress-crazing. A quick literature search revealed that stress-crazing is part of a larger subject known as stress-cracking and that:

- Considerable literature is available on stress-cracking;
- The literature is somewhat contradictory;
- Most of the literature concerns metals, although several good sources of information on plastics and polycarbonates were discovered;
- Stress-cracking (and stress-crazing) can occur in many plastic materials, especially polyamides, acrylates, polycarbonates, polystyrene, polythene, acrylonitrile, and polyethylenes,[2] and that polyethylenes and polycarbonates show the most pronounced stress-cracking;
- Stress-cracking is an extremely complex phenomenon and its mechanism is not yet completely understood in either metals or plastics;
- Stress-cracking can be caused by solvents, environments, mechanical stresses, thermal stresses, oxidation effects, and electro-mechanical effects;
- Stress-cracks can be caused by uniaxial or polyaxial stresses; and
- Carefully controlled experiments to produce valid useful data are required.

After the preliminary literature search, a broad investigation on stress-cracking of polycarbonates was proposed by W. J. Stone to J. Daly, February 5, 1970, and was approved. The purpose of the investigation was

to develop an experimental design for a general investigation of stress-cracking phenomena for any material. As a result, Phases I and II, as defined by Materials Engineering, involved subjecting injection-molded specimens to dead-loads over a period of time while the specimens were subjected to 50 and 100 percent relative humidities. Progress on this project from May 11 through June 5, 1970, is reported in Stress-Cracking of Polycarbonates.[1] In this investigation, basic mechanical properties of polycarbonate material were established through tensile, creep, and impact tests. Tensile properties at +165°F were also investigated. It was shown that annealing raised the ultimate strength approximately 15 percent but lowered the yield strain approximately 15 percent. The effects of specimen bulk and design geometry on mechanical properties were examined by a series of tensile, creep, and fatigue tests. To this point, the tests indicated that varying bulk, geometry, and stress concentration had no significant effect on stress-cracking susceptibility for tensile loads under the yield strength, except in fatigue where biaxial stresses considerably reduced fatigue life. Stress-cracking was induced in specimens by tensile, creep, and fatigue loading. Optical methods, such as photoelasticity, dark field projection, and standard immersion fluids were used to study cracks and stress patterns. Surface residual stresses in injection-molded specimens were measured by the General Electric method of immersing specimens in a 50:50 solution of methanol and ethyl acetate and found to be 2000 psi.

The Phase I and II specimens which were dead-loaded (creep) in room air and in air at 100 percent relative humidity showed no stress-cracks after 750 hours. However, the brittle failures which occurred in fatigue and biaxial tension tests indicated that stress-cracks could be a problem when fracture toughness is significant, such as in stress concentrations, biaxial stresses, and large deflections. Fracture toughness tests were run and brittle fractures obtained. The tests predicted a critical crack length of 0.156 inch for polycarbonate. Voids 0.014 to 0.018 inch in diameter were discovered in many injection-molded tensile test specimens shortly after they yielded during standard tensile tests. It was concluded, therefore, that stress-cracks in polycarbonate are significant and that they should be taken into consideration in the design of parts made from polycarbonate material.

ACTIVITY

Stress-Cracking Factors Described

Stress-Cracking Defined

The terms stress-cracking and stress-crazing are often used interchangeably. Stress-crazing is considered a surface effect only, whereas stress-cracking occurs both internally and on the surface. Figure 1 shows typical stress-cracks in polycarbonate. A stress-crack is formed when a material starts to yield locally under load. The stress-cracks in Figure 1 were readily

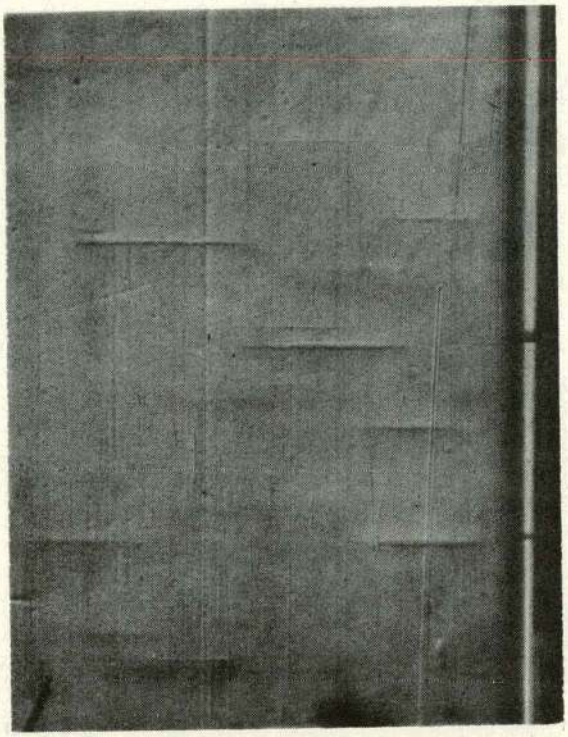

Figure 1. Typical Stress-Cracks (Horizontal Lines): Load Axis Is Vertical (50X)

obtained by creep (dead-load) testing. These cracks are internal and well developed and, like all stress-cracks, are perpendicular to the principal stress axis.

Polycarbonate Failure Mechanisms

Polycarbonate is considered strange material because of the manner in which it fails. It is very ductile, yet stress-cracks at tensile loads which are only 60 percent of the yield stress. It can be stretched 60 to 140 percent, yet will fail in a brittle manner under less than 1-percent strain. Unlike metals, it can be strengthened by annealing. To understand stress-cracking and fracture toughness in polycarbonate, it is necessary to know how polycarbonate fractures. Polycarbonate fails by several different mechanisms which are actually ways of adjusting to loading so as to resist failure. Two types of loading--tension and stress-cracking--will be used to illustrate those mechanisms which determine how test specimens fail.

Uniaxial Tensile Loading

Depending on its processing, polycarbonate yields in an unusual manner at 5 to 15 percent strain. Under tensile loading, yielding progresses as two wave fronts in the box specimen traveling rapidly in opposite directions along the gage length. The material yields by "thinning" as well as "narrowing" in width as much as 25 percent. The wave fronts travel up the shoulders until they reach a point where narrowing in width ceases. Meanwhile, the material continues to thin in the shoulders by an additional 1/4 to 1/3 inch. A few voids may appear on the surface or internally while this is happening, and the yielded material whitens if specimens are transparent. At this point, brittle fracture usually occurs in the gage length, sometimes where the material is several thousandths of an inch thinner, or at a void, or where the gage length was touched by a human hand.[2] Stress-cracks normally do not appear.

The whitening of a transparent polymer is called a "blush."[3] Blushing usually starts at the surface of a specimen, if no residual stresses are present, and penetrates the interior. Although little is known about blushing, it is probably not related to crazing since it will not "heal" itself as will crazing. Blushing should not be confused with the formation of spherulitic crystalline growth during cold drawing since it can occur in the absence of a crystalline structure.

The voids appear during this pronounced plastic flow period because of the separation of layers of molecules which are normal to the plane of the applied stress, whereas molecular reorientation, similar to that during cold drawing, is taking place.[4] The molecular chain activity consists of a realignment of large chain segments in a direction normal to the shear gradient and is accomplished during cold flowing by the van der Waal bond forces of adjacent molecules.[5] This allows the occasional sudden appearance or opening of a void. Because of this activity, during the plastic flow the material is strain-hardening and behaves more like a metal than a conventional inorganic glass. The strain-hardening prevents fracture at a void, or local defect, during plastic flow. Brittle fracture occurs after molecular rearrangement is essentially complete.

Craze Matter

Typical polycarbonate stress-cracks are shown in Figure 2. As shown by microscopic examination and electron photomicrographs of microtomed stress-cracks in polymers, stress-cracks or crazes are not empty voids.[6, 7] They are filled with a material called "craze matter" which is anisotropic to the parent material, and has a striated texture oriented along the craze width parallel to the tensile load axis. Craze matter can support crack propagation normal to its own crack.

Studies of polycarbonate material show that the crazes (voids) are 50 to 60 percent polymer with a porous structure. The tiny pores vary greatly in size and are randomly distributed throughout the craze material. The longest and fewest cracks occur at the lowest stress levels in polymers. At room temperature, stress-cracking occurs by cold flowing, and has three phases: initiation, progression, and termination.

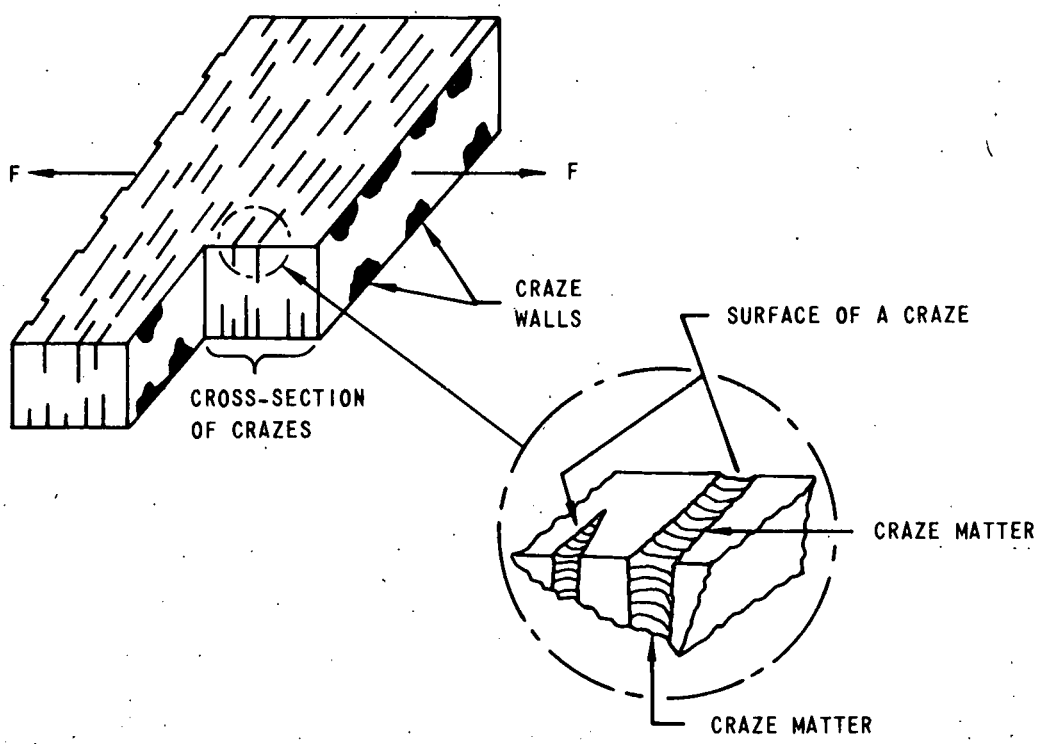

Figure 2. Typical Polycarbonate Stress-Cracks Showing Deformed (Realigned) Craze Matter

Crack Initiation

In the initiation phase of stress-cracking, energy supplied by tensile loading builds, causing molecular redistributions or rearrangements to occur at the site of defects and nonhomogeneities. There is movement of polymer chains in the direction of the applied tensions. This action results from the fact that bodies containing large asymmetric molecules have a mesomorphic (semi-crystalline) state generated during a pronounced inelastic shear by a mechanism of chain segmental diffusion. A net realignment of polymeric chains in a direction normal to the shear gradient occurs and a new state of aggregation occurs as the material becomes oriented differently to the parent material.

Crack Progression

Once molecular segments of the material attain some critical pre-disposition to the direction of the tensile force, a crack starts to develop. The crack propagates by the yielding and cold flowing of the resin at the periphery of the crack. The ability of the resin to undergo this deformation apparently depends on its lubricity and molecular weight. The lubricity affects diffusion and requires a finite amount of time which generally is large enough to prevent the appearance of stress-cracks during a tensile test. Relief of the stress at the initiation site causes adjacent regions to become more highly stressed in a plane perpendicular to the tensile load. The adjacent regions are then converted to craze matter. The tip of the stress-crack is composed of resin which is also converted to craze matter; small incremental stresses are sufficient for this conversion. The path and shape of the craze periphery depends on the randomness or orientation of the surrounding resin which is being acted upon by these stresses.

Crack Termination

Despite its stress-cracks, a specimen will continue to support a tensile load for a long time. However, resin around the stress-crack undergoes oblique flow. This action permits eventual redistribution of the local stress to a negligible level at the craze-crack surface so that the incremental microscopic creep can no longer sustain significant craze propagation. This type of creep is not the same as the creep which causes delayed and necked fracture. Small stress-cracks (stars especially) will disappear because of local molecular chain movement. Ultimate rupture may or may not occur through a true craze-crack. If it does, failure appears to be in the bond between the craze matter and the crack surface. Stress-cracks can coalesce after a time and can cause ultimate rupture. However, failure can also occur through true voids which arise from a major defect like those mentioned in the description of the tensile failure mechanism.

Stress-Crack Evaluation

All work accomplished to date was designed to evaluate polycarbonate stress-cracking by:

- Inducing stress-cracking
- Determining when and where stress-cracks occur; and
- Relating stress-cracking to existing engineering material design parameters.

In the first period of testing, the first two items were accomplished. The second period of testing was devoted to the third item. Phases I and II creep (dead-load) tests were continued, and the elastic limit of polycarbonate was

Table 1. Phase I and II Creep Tests: Status as of 12 p.m., January 30, 1971

Group	Date Specimen Loaded	Test Atmosphere	Load Level		Elapsed Time at Load Level (hr)	Remarks
			(lb)	(psi)		
1	May 11, 1970 10:00 a.m.	Room	290	4,640	6,338	No visible cracks
2	May 11, 1970 10:00 a.m.	Moist	290	4,640	6,338	First crack noted on July 9, 1970 at 1,248 hours: Many large cracks currently visible
3	Dec. 11, 1970 1:00 p.m.	Room	315	5,040	1,199	No cracks
4	Dec. 11, 1970 1:00 p.m.	Room	340	5,440	1,199	First crack noted on Dec. 17, 1970 at 144 hours: Several small cracks currently visible

determined. The effects of annealing polycarbonate in an inert atmosphere were studied, as were the variables affecting fracture toughness of polycarbonate.

Phases I and II Creep Tests

Testing continued on the two strings of injection-molded specimens loaded as shown in Figure 3. Specimen dimensions are shown in Figure 4 and test results are given in Table 1. Specimen Groups 1 and 2 have accumulated 6338 hours as of January 30, 1971, at 5883 psi. No visible cracks have appeared in the Group 1 specimens hanging in room atmosphere. A stress-crack was found on July 9, 1970, in the lowest specimen of Group 2 tested in moist atmosphere at 1248 hours or approximately 59 days after loading. At the time of this writing, several dozen cracks have appeared and have grown to large size. Some cracks are about 80 percent of the 0.125-inch thickness, while others are now one-half of the 0.5-inch width. This specimen is predicted to fail eventually. The specimen next above also developed stress-cracks. It was concluded, therefore, that the moist atmosphere created by bubbling air through water is affecting stress-cracking.

Therefore, on December 11, 1970, Groups 3 and 4 specimens were dead-loaded at higher loads in room atmosphere to provide more data points as a base line. The new loads of 5040 and 5440 psi are 60 and 65 percent of the yield strength. At 144 hours, a stress-crack appeared in the specimen loaded to 70-percent yield stress. At 1199 hours it had several small cracks.

Elastic Limit Determination

Since the elastic limit of polycarbonate is not yet published, seven injection-molded specimens similar to that shown in Figure 4 were tested to establish the elastic limit magnitude. Results are shown in Table 2.

Table 2. Elastic Limit of Polycarbonate Lexan 131 Injection-Molded Specimens

Specimen	Elastic Limit (psi)
1	4330
2	4600
3	4760
4	4850
5	4700
6	4620
7	4620

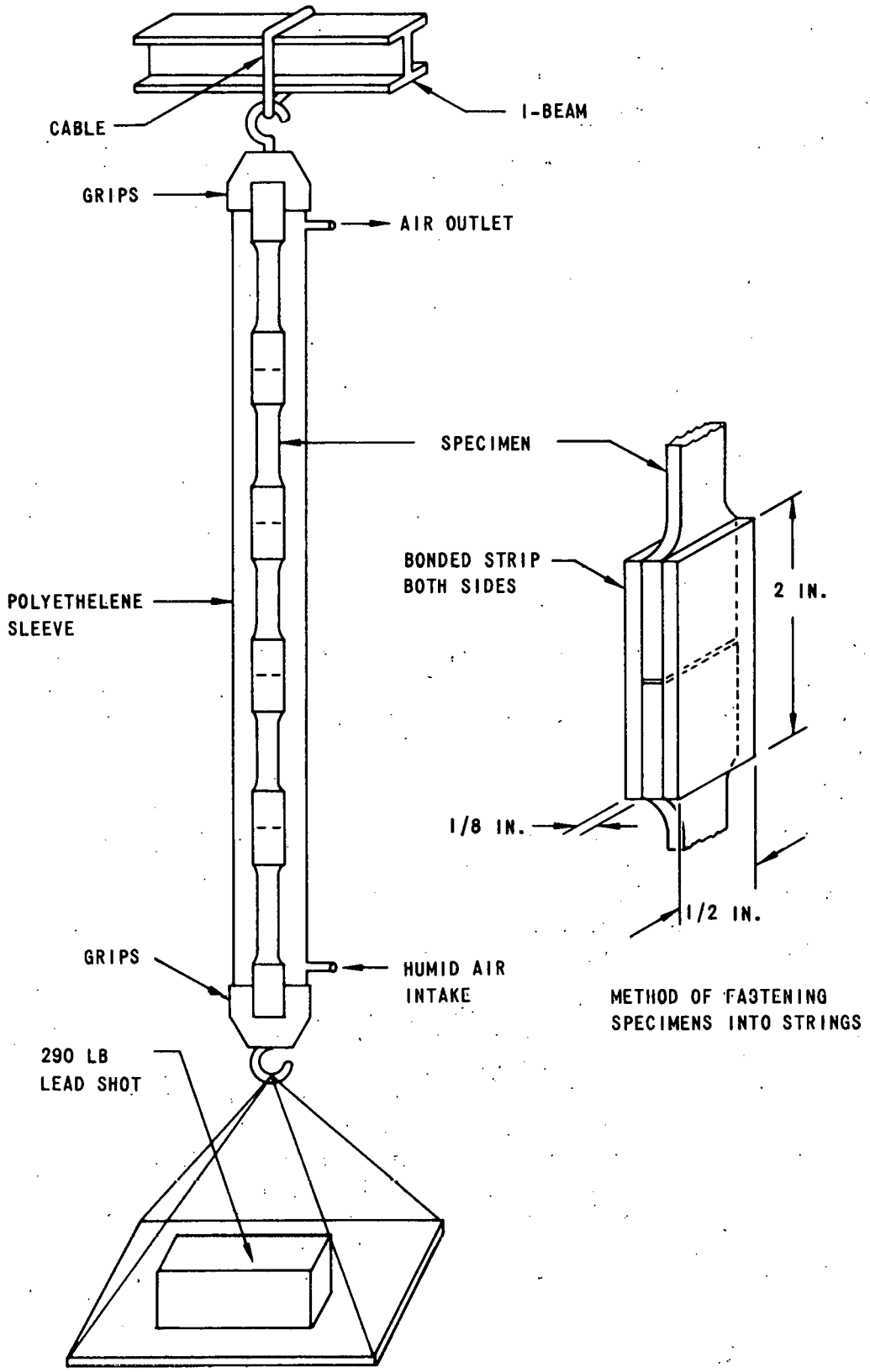

Figure 3. Dead-Load Test Setup for Phases I and II Polycarbonate Stress-Cracking

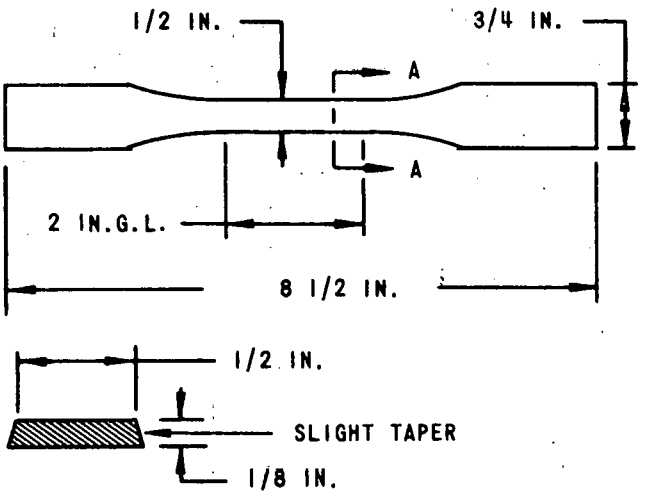

Figure 4. Standard Tensile Specimen

The average of all specimens gives an elastic limit of 4600 psi, ± 3 percent. The strain rate was 0.2 inches per minute. This information is needed for studies of fracture toughness, residual stresses, low cycle plastic strain, and polyaxial stresses.

Residual Stresses

Previous calculations indicated surface residual stresses could be over 2000 psi.[8] Therefore, several more annealing studies were made using Lexan 131 since General Electric and Mobay Incorporated recommend a design stress of 1000 psi for polycarbonate in repeated loading.[9, 10] General Electric further recommends 800 psi for long life in repeated loading.

A two-by-two factorial experiment was run in which specimens were annealed in an argon atmosphere. Standard injection-molded Lexan 131 specimens as shown in Figure 4 were annealed at 320 and 380°F for periods of 2 and 100 hours. A quick stress analysis showed that a cooling rate of 60°F per hour recommended by the manufacturer could easily cause a thermal stress of 1000 psi in a 1/8-inch-thick specimen. Therefore, specimens were cooled after annealing at a rate of 15°F per hour. The 380°F specimens developed bubbles, which were believed to be moisture, and were discarded. The 320°F specimens which were annealed for 100 hours were tensile-tested along with two as-molded specimens for comparison. Test results are shown in Figure 5 and Table 3.

A striking increase of approximately 42 percent in the yield strength is evident. A 31-percent increase in yield strength was obtained from Merlon 50 specimens annealed in air.[1] The yield strain was reduced approximately 18

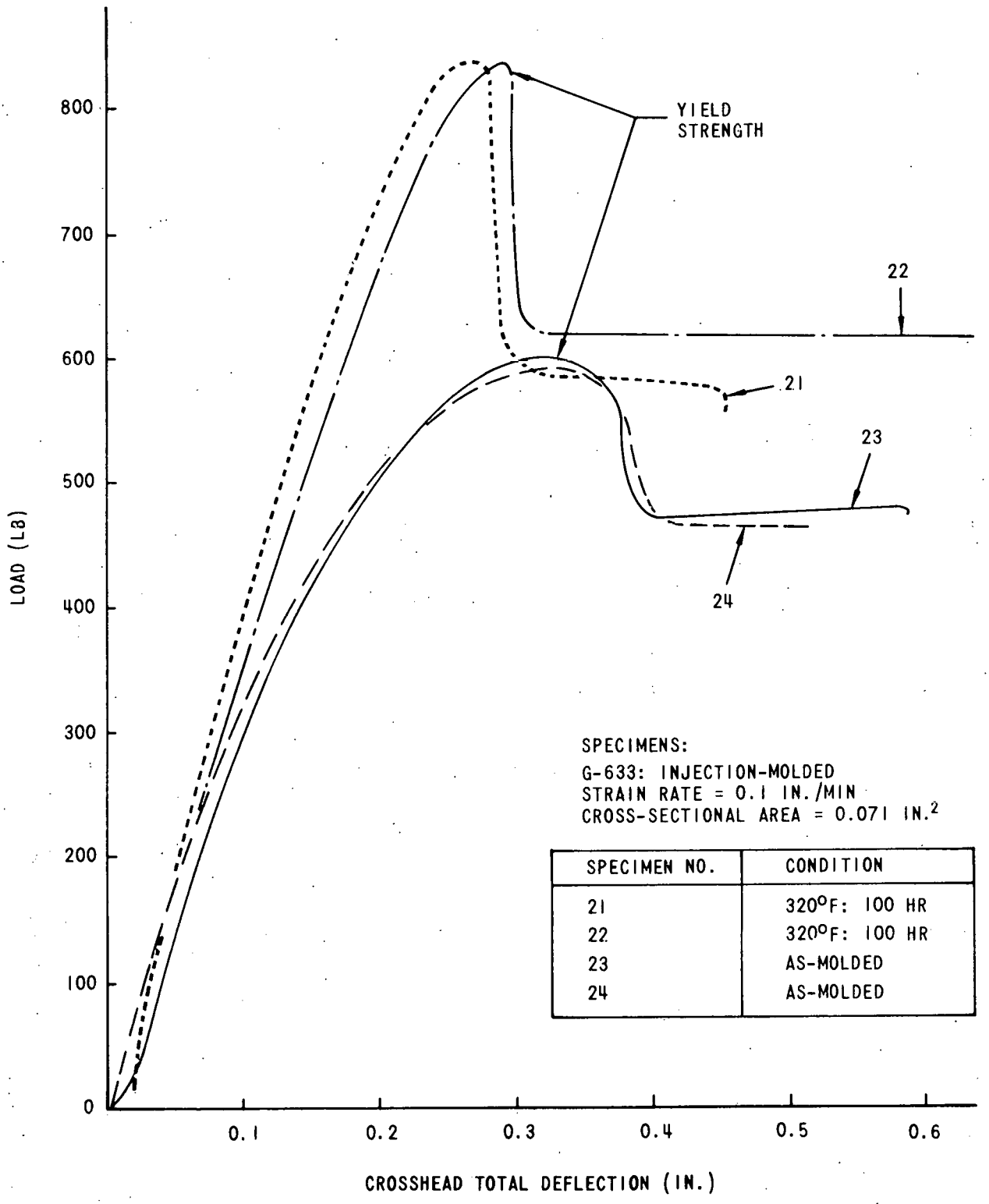

Figure 5. Effect of an Inert Atmospheric Anneal on Lexan 131

percent. Since the 250°F, 5-hour-per-inch thickness anneal recommended by the manufacturer caused no appreciable reduction in photoelastic fringes in previous tests, 320°F was used since it is the Vicat softening temperature (ASTM-D-1525-58T) which is just above the 300°F glass transition temperature of polycarbonate as stated in the Mobay brochure. Although the specimen shrank 15 percent in length, the argon atmosphere eliminated the yellow discoloration observed in past anneals. The many photoelastic fringes observed in as-molded specimens were removed with only one-half fringe remaining. Annealed specimens showed no change in X-ray diffraction patterns of density.

Table 3. Effect of an Inert Gas Atmosphere Anneal on Lexan 131

Specimen	Load (lb)	Yield Strength (psi)	Yield Strain* (in./in.)	Remarks
21	832	11,718	0.137	Annealed
22	830	11,690	0.146	Annealed
23	590	8,310	0.163	As-molded
24	580	8,169	0.169	As-molded
*Strain between crossheads, 2-inch-gage length				

A literature search was made for methods of measuring residual stresses. No established photoelastic methods were found, although it appears photoelasticity may eventually embrace residual stress studies.

In a further study of residual stresses in injection-molded parts, an aluminum fixture (Figure 6) was made which holds four parts and physically restrains the parts during annealing in argon. Using this fixture, four specimens were then annealed at 300°F for 144 hours to study effect of preventing shrinkage of specimen upon residual stresses. Shrinkage was reduced to 5 percent, compared to 15 percent on unrestrained specimens. Only one-half of a photoelastic fringe remained, and most of the shrinkage was around the molding sprue. The four specimens will be compared with as-molded specimens using tensile and dead-load tests. The stresses possibly have been realigned axially. A proposal for a separate study of residual stresses has been outlined and submitted.

Extruded Polycarbonate

In the previous reporting period, extruded and annealed rods and sheets were procurred to test thicker specimens for fracture toughness and other material properties. At that time it was reported that the 1/4-inch-thick sheet was

free of photoelastic fringes and possibly even stress-free (bottom specimen, Figure 7), whereas the rest of the material contained many fringes. It was discovered that the 1/4-inch sheet was manufactured by the General Electric Corporation, but the rest was supplied by Westlake Plastics Incorporated. An infrared spectroscopic analysis proved the material was polycarbonate. Its stress-free appearance should be investigated.

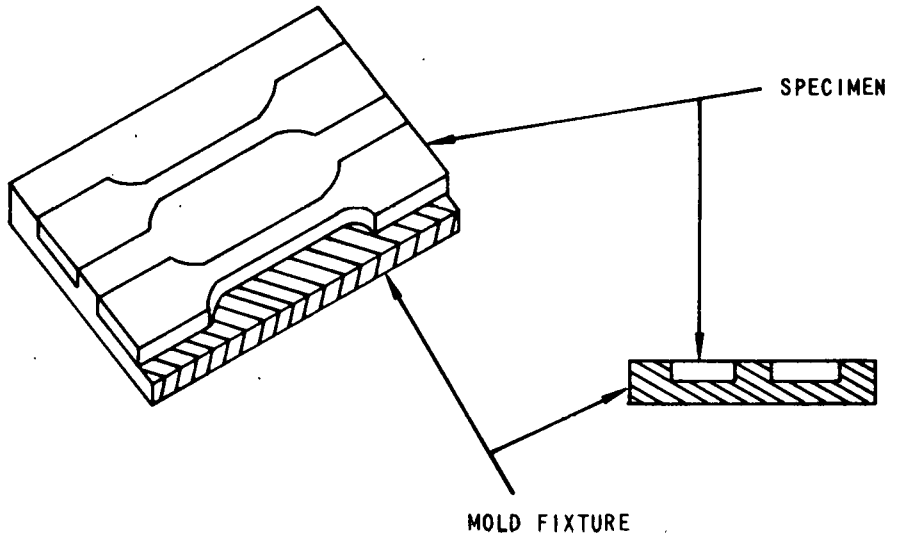

Figure 6. Aluminum Annealing Fixture Showing Method of Restraining Specimens

Fracture Void Investigation

It was previously reported that during tensile testing, voids appeared in the gage length shortly after specimens started to yield. The voids were 0.014 inch in diameter and larger, and fracture usually occurred through one of them. The voids were noted in Merlon 50 and Lexan 141 specimens. Since stress concentrations can raise design stresses above the yield strength in local areas, it was felt that these voids needed further study. Also, it was hoped that these voids could be used as an independent check on fracture toughness constants for polycarbonate. A study of these voids was started by tensile testing 12 specimens while carefully checking visually for the appearance of voids. No voids appeared on the specimens tested, which may be because they were Lexan 131. This study was discontinued when the project was terminated.

Fracture Toughness Investigation

In the discussion of polycarbonate failure mechanisms, it was pointed out that well developed stress-cracks are filled with a realigned craze material which contains many tiny voids, and that stress-cracks can eventually grow, coalese,

THIS PAGE

WAS INTENTIONALLY

LEFT BLANK

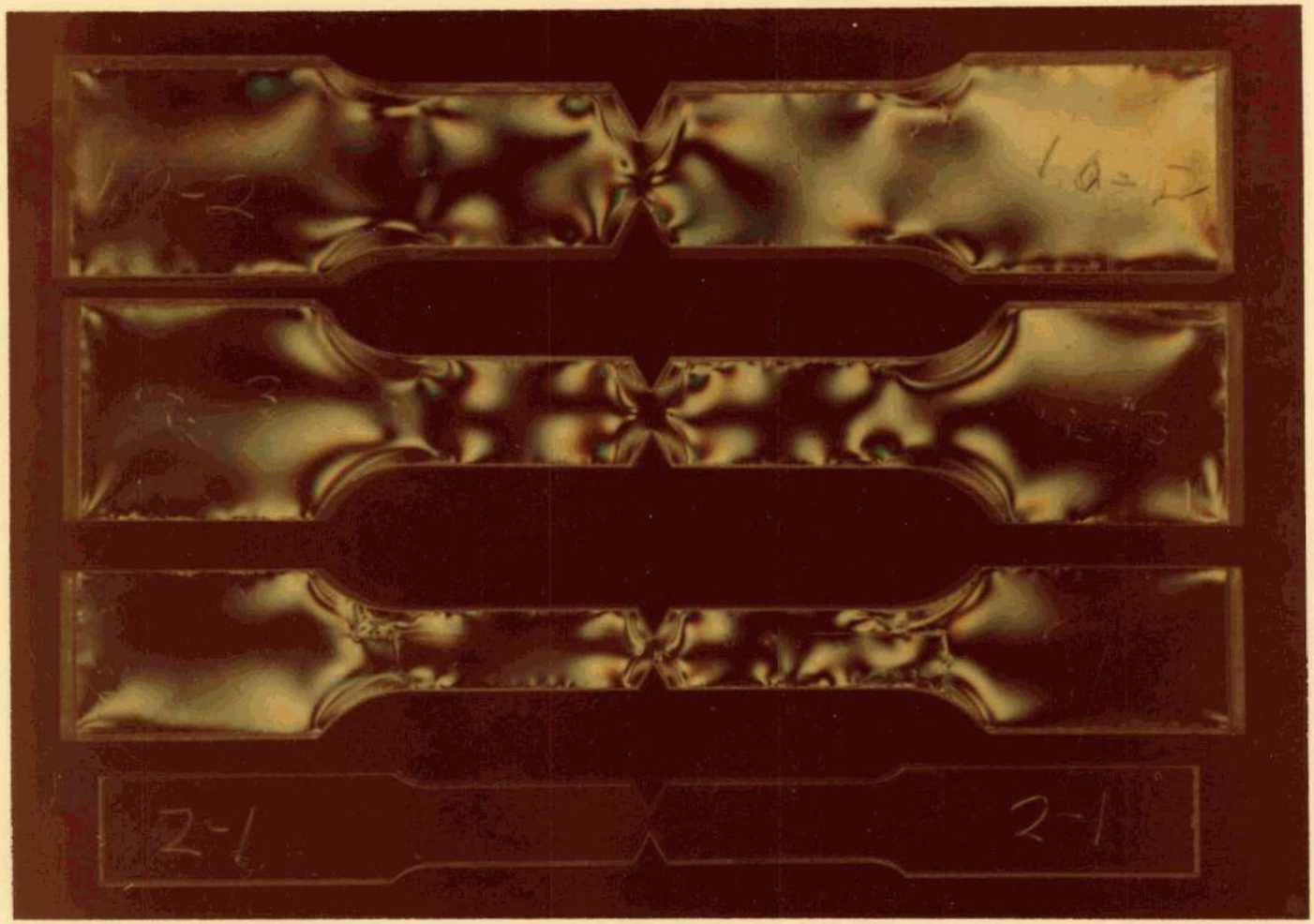

Figure 7. Photoelastic Patterns of Specimens of Test Series 5 and Test Series 3 (Bottom Specimen)

THIS PAGE

WAS INTENTIONALLY

LEFT BLANK

and cause rupture in the parent material.[11] Based on experience with creep and low cycle fatigue specimens, it is now believed that stress-cracks produced in the Bendix Test Laboratory are also filled with a craze material because stress-cracked specimens continue to support loads greater than can be justified, even by strain-hardening. In addition, the biaxial fatigue specimen, reported in Stress-Cracking of Polycarbonates, failed in a brittle manner in the presence of stress-cracks. Its fatigue life of 17,880 cycles was considerably shorter (40 percent) than a uniaxial fatigue specimen of 30,000 cycles. This result indicated that serious cracks can develop in polycarbonate parts.

Since it is now believed that stress-cracks will appear in service parts, the concept of fracture toughness was examined. It was concluded that the concept of fracture toughness can be used to predict what crack length in a given part will produce sudden catastrophic failure. This concept is explained briefly in Appendix A. The fracture toughness theory has come into engineering use within the last two or three years. As yet, very little data on polymers is available, and the existing data for predicting the critical size of stress-cracks is incomplete.

Injection-Molded Material

The normal ductility of polycarbonate would produce sufficiently good fracture toughness that a simple fracture toughness test would establish the constant, K_{Ic} (plane strain fracture toughness) for polycarbonate.[12] Therefore, in the previous reporting period, a fracture toughness specimen was designed (Figure 8).

Seven specimens were machined and tensile-tested until they failed by sudden crack propagation. The test results are shown in Table 4. Specimens were made of injection-molded, 1/4- by 1/2- by 5-inch bars. The notch was designed using Bowie's formula (Appendix A) and ASTM-STP-410.[10] The notch radius is considerably smaller than that necessary to simulate a crack. The notch itself was designed to give as brittle a fracture as possible since polycarbonate is so ductile. This was done by using a small cross-sectional area to keep the plastic zone small. This method allowed a deep notch root to ensure plane strain fracture. Machining the notches added two photoelastic fringes (approximately 350 psi residual stress).

Three strain rates, 0.005, 0.2, and 0.5-inch-per-minute of crosshead travel, were used. There was no significant difference in failure load, as shown in Table 4. The test results were used to calculate a K_{Ic} and 3,050 psi $\sqrt{\text{in.}}$ was obtained using Bowie's formula:

$$K_I = \frac{YPa^{1/2}}{BW}$$

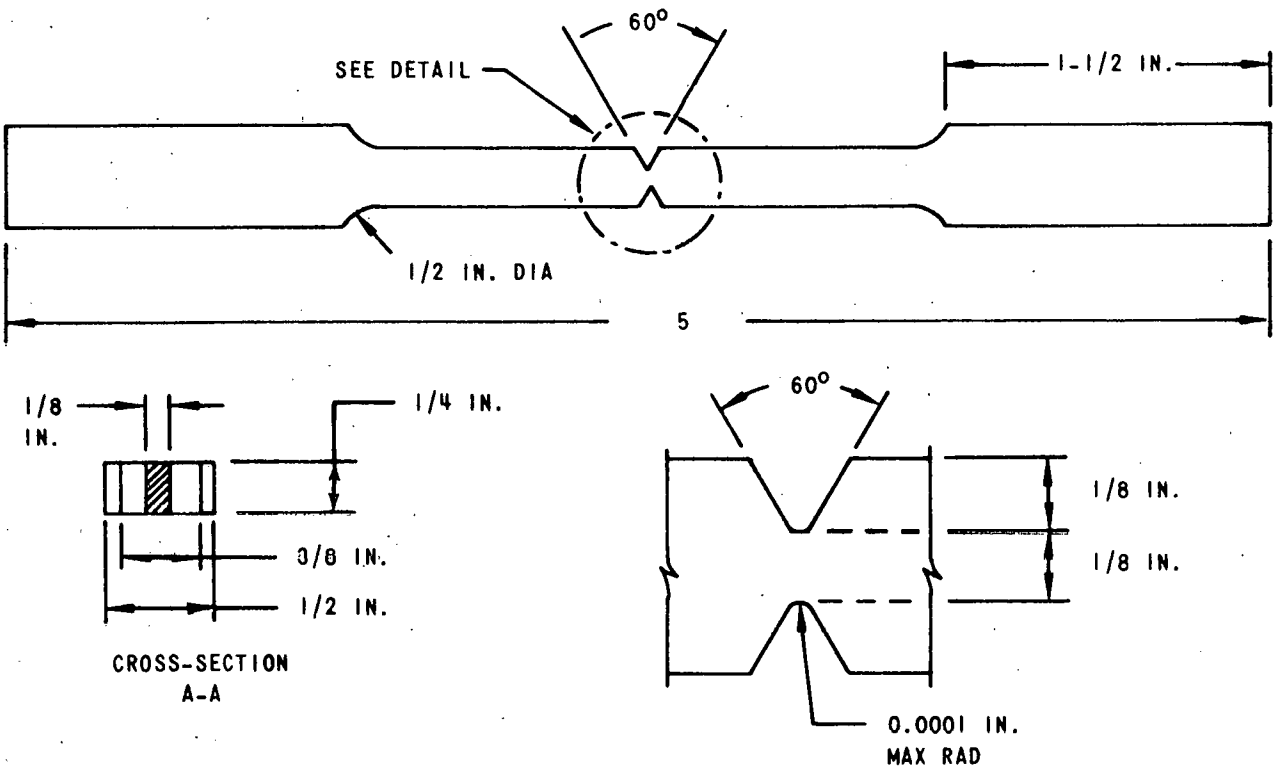

Figure 8. Fracture Toughness: Notched Tensile Specimen

Table 4. Fracture Toughness: Lot G-633, Lexan 131

Specimen	Failure Load (lb)	Failure Load (psi)	Strain Rate* (in./min)
1	325	5,200	0.200
2	325	5,200	0.200
3	325	5,200	0.200
4	330	5,290	0.500
5	327	5,232	0.200
6	320	5,120	0.050
7	**	**	**
8	322	5,152	0.200

*Crosshead speed
**Broke in assembly

where:

K_I = Plane strain intensity factor (psi $\sqrt{\text{in.}}$);

Y = 2.3, a geometric constant from Figure 5, p. 10 of ASTM-STP-381 (in.^{3} per pound);

P = Fracture load (lb);

B = Specimen thickness (in.);

W = Specimen width (in.); and

a = Crack depth (in.).

Using Irwin's formula (Appendix A) and a stress level of 7700 psi (selected because it is just below yield in dead-loading) for polycarbonate, a critical crack length for stress-cracks was calculated to be 0.156 inch. Since most stress-cracks at that time were approximately 0.015 inch, this amount would appear to indicate a safe fracture toughness situation. However, the test laboratory has now obtained longer cracks at lower stress levels. An inspection of the load-deflection curves in Figure 9 showed that some plastic flow must have taken place in the test specimen. The broken line curve in Figure 9 was expected, but the solid line or actual curve was obtained instead. Fracture should occur abruptly. A well-rounded curve indicates insufficient thickness, as seen in Figure 26, page 41 of Brown and Strawley, or plastic flow at the edges, or a relatively large plastic zone ahead of the advancing crack tip. An examination was made of fracture surfaces of the test specimen (Figure 10). Two plastic flow areas which were about 0.015-inch high at the corners and tapered to zero height at the center were found. A hemispherically concave nick approximately one-third the specimen width appeared at each specimen face.

Since a considerably lower value of K_{Ic} had been expected, the specimen design details were rechecked and found to conform to the recommended design practice stated in ASTM-STP-381, and ASTM-STP-410. Four independent stress calculations indicated that the specimen width, thickness, notch depth, notch radius,[14] and cross-sectional area[15] should be more than satisfactory.

A study of available literature showed that the "plastic flow tongues" result from plastic flow at the face of the specimen which tapers off to zero in the center because of the restraint of adjacent material.[16] It is also pointed out that plane strain fractures can still occur under these conditions since plane strain obviously occurred in the center of the specimen at fracture as well as in the notch radius. Tetelman and McEvily point out that if triaxial loading occurs in a thick ductile specimen, small transverse contractions will

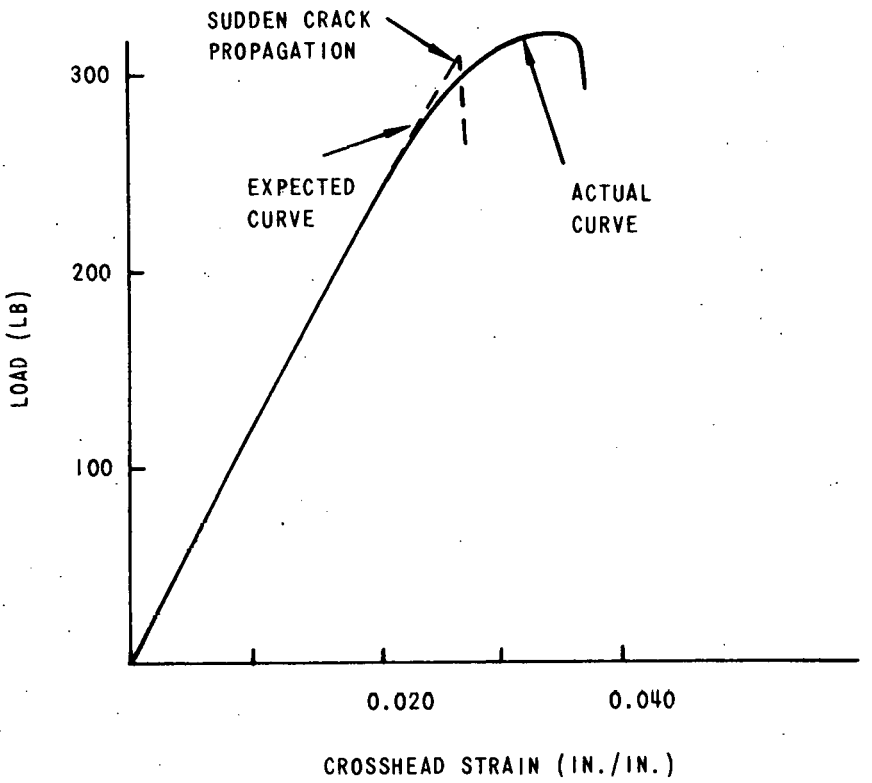

Figure 9. Typical Load-Deflection Curve for Fracture Toughness Test, Series 2

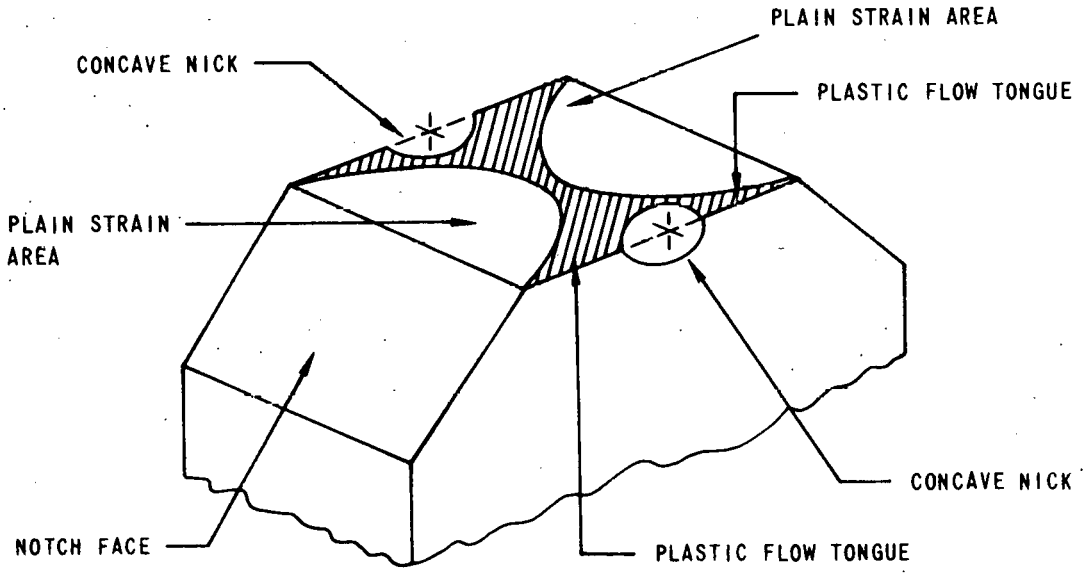

Figure 10. Typical Fracture Face

occur near the tip of the notch. The nick on each face of the specimen indicates that triaxial loading occurred. Summarizing the results of this test, brittle fracture apparently was obtained, but was affected to a small extent by the plastic flow that occurred.

Annealed Sheet Material

Since Sippel and McEachen indicated that processing could affect fracture toughness, a third test series was machined to the same specimen configuration as was Series 2 using the General Electric annealed 1/4-inch sheet (Figure 8). The object of this test was to compare the somewhat less ductile annealed and extruded sheet with the injection-molded material.

Specimens were tensile-tested on a 10,000 pound Instron tensile tester at a strain rate of 0.4 ipm crosshead speed. Test results given in Table 5 show a decrease of approximately 27 percent. This decrease indicated less plastic flow before fracture, as Figure 11 shows. The sharp peak also indicates a sudden catastrophic crack propagation. The annealed material curve peaks just before fracture, which could indicate plastic flow of material in the general area of the notch and/or plastic flow of the material ahead of the advancing crack tip. A plane strain plastic zone correction factor, called a "plastic compliance factor," for plastic flow ahead of the crack tip, can be used to give a more accurate value for K_{Ic}. Irwin's correction factor was used.[17,18]

This correction factor adjusts the critical crack length as follows:

$$a_1 = a_o + \frac{1}{3\pi} \frac{(K_I)^2}{(\sigma_{y.s.})^2}$$

where

a_1 = Corrected critical crack length (in.);

a_o = Critical crack length calculated from K_{Ic} (in.);

K_I = K_{Ic} obtained experimentally (psi $\sqrt{\text{in.}}$); and

$\sigma_{y.s.}$ = Yield strength of the material (psi).

This factor was used to determine a corrected K_{Ic} as shown in Table 6. The difference is less than 4 percent.

Table 5. Fracture Toughness Test Series 3: General Electric Lexan 141, Fully Annealed Sheet

Specimen	Failure Load (lb)	Failure Load (psi)*	K_{Ic} (psi $\sqrt{in.}$)
2-1	295	3,148	2,670
2-2	250	2,667	2,270
2-3	222	2,368	2,000
2-4	235	2,506	2,130
2-5	255	2,720	2,320
2-6	285	3,040	2,670

*Based on gross cross-sectional area

Table 6. Fracture Toughness: Annealed Lexan 141

Specimen	K_I (psi $\sqrt{in.}$)	K_{Ic} (psi $\sqrt{in.}$)	Brittle Fracture Surface (Percent)	Good Initial Brittle Fracture	Multiplane Fracture	Critical Crack Length (in.)
2-1	2,670	2,771	40	Yes	Yes	0.087
2-2	2,270	2,324	35	Yes	Yes	0.061
2-3	2,000	2,058	40	Yes	No	0.048
2-4	2,130	2,179	50	Yes	No	0.054
2-5	2,320	2,371	25	No	Yes	0.064
2-6	2,570	2,671	30	No	Yes	0.071

Brittle fracture initiation apparently was obtained, but because some plastic flow occurred, specimen fracture surfaces were examined under a binocular microscope.

The percent of specimen surface which fractured in a brittle fashion was visually estimated and given in Table 6. Although no surface showed more than 50 percent brittle fracture, plastic flow occurred on less than 5 percent of each fracture surface. The remaining specimen surfaces were composed of debris which is typical of brittle fracture surfaces and results from large amounts of energy being released suddenly ahead of the advancing crack tip. This release causes secondary cracks to form, resulting in multiplane

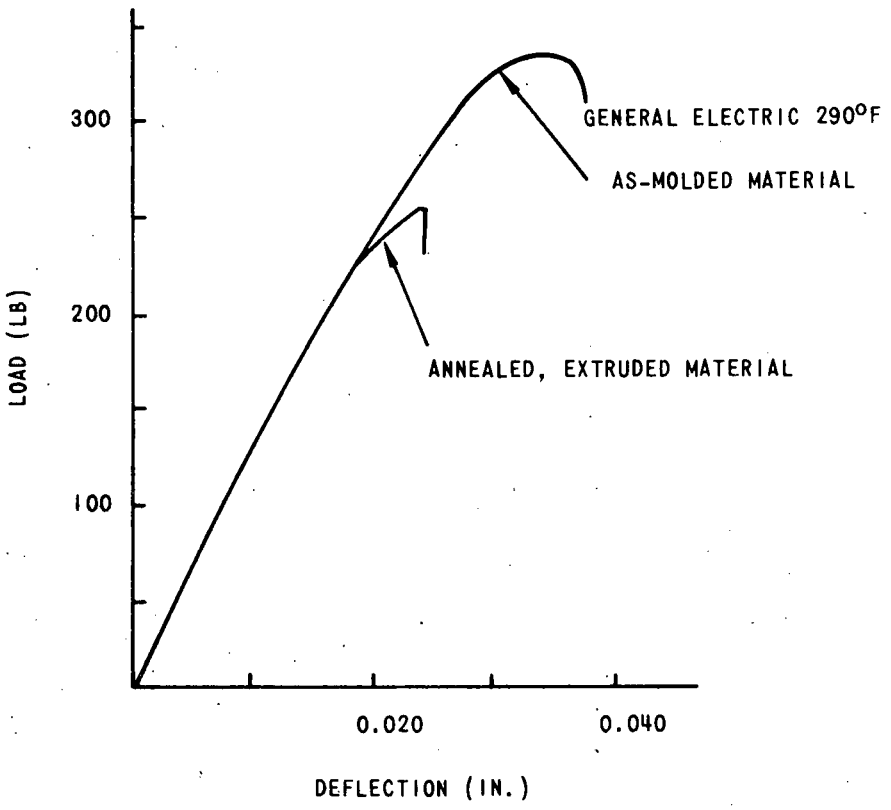

Figure 11. Comparison of Load-Strain Curves

fracture surfaces, and indicates a plastic zone ahead of the crack tip. Note that Specimens 2-3 and 2-4, in Table 6, which have the lowest K_{Ic} values, had almost no brittle fracture surfaces. Yet both had a multiplane step in the fracture surface as did all the other specimens. The step appeared because each specimen failed at one notch first, and, as the crack propagated, the specimen bent slightly because of the resultant, increasingly unbalanced axial load. This action caused the first crack to change direction slightly and miss the second crack advancing toward it, which shows that crack propagation was obtained (rather than a general tensile failure) despite the narrow width of the specimen.

The crack in Specimen 2-6, Table 6, started as a ductile tear. The crack in Specimen 2-5 started when a ductile plug sheared vertically out of one fracture surface near the notch root. The plug was approximately 0.05 by 0.45 inch in cross-section. The surface of Specimen 2-3 had the most brittle fracture as well as the lowest K_{Ic} value. Using Irwin's formula, critical crack lengths were calculated and found to range from 0.048 to 0.071 inch for a stress level of 5300 psi, which is the lowest stress level at which stress-cracks were observed in dead-load tests.

Because of the different plastic effects mentioned, it was felt that wider specimens of the same material would produce a smaller critical crack length for the same material condition. Thicker specimens will also result in a lower K_{Ic} and smaller critical crack size. Although the values for K_{Ic} and critical crack size are valid, it is recommended that additional tests be made for different widths and thicknesses because polycarbonate fracture toughness is apparently influenced by geometry in the same manner as metals.

Unannealed Sheet Material

The basic notch design was again reviewed and found to be satisfactory. The special purpose notches, such as the chevron edge crack notch for bending and the pre-cracked center crack notch for fatigue have, to date, proved no better than the plain edge notch, as Sippel and McEachen point out. The specimen design and dimensions are shown in Figures 12 and 13. A larger thickness was used to study the effect of bulk, and the net section width was increased and varied (Table 7) to reduce edge effects and to study the ratio of notch depth to specimen width (2a/W).

Five specimens of each size were machined and tested. The top three specimens of Figure 7 show the birefringent patterns on one specimen of each size. Note the fringes in the vicinity of the notch. These are caused by residual stresses resulting from machining.

Table 8 presents the results of specimens tested in an Instron universal tensile tester. Plane strain fracture toughness values (K_{Ic}) were calculated

Table 7. Fracture Toughness Specimen Design Variables: Test Series 4

Design Identification	Notch Depth (in.)	Gross Width (in.)	Net Notch Section Width (in.)	Net Cross Sectional Area ($in.^2$)	Notch Depth To Specimen Width Ratio $\frac{2a}{W}$
A	0.225	0.750	0.300	0.150	0.6
B	0.150	0.500	0.200	0.100	0.6
C	0.125	0.375	0.125	0.0625	0.67

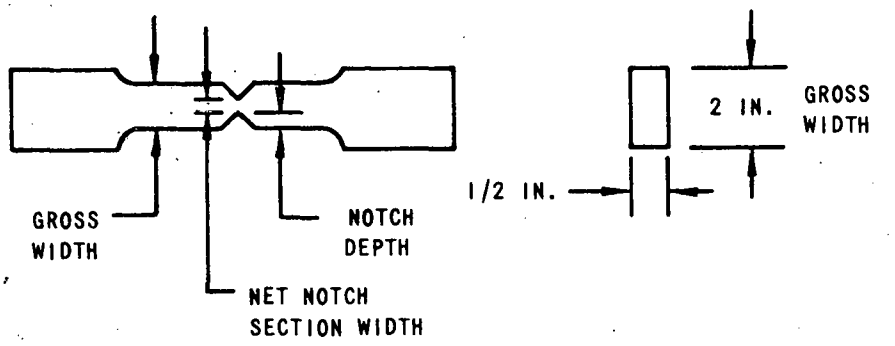

Figure 12. Fracture Toughness Specimen Design

and then corrected with Irwin's plastic compliance factor for plastic flow at the crack tip. These values range from K_{Ic} = 1412 psi $\sqrt{in.}$ to 3307 psi $\sqrt{in.}$ but 11 of the 15 are considerably lower than those of Test Series 3, Table 6. The lowest (1412) predicts a critical crack length of 0.021 inch (based on a stress level of 5300 psi, which is the lowest stress level at which cracks were observed in dead-load tests), whereas all but four predict a critical crack length of less than 0.040 inch. This fact indicates that stress-cracks in polycarbonate can be extremely detrimental to polycarbonate parts.

Since there is a large range in the predicted critical crack sizes from 0.021 to 0.123 inch, the fracture surfaces were examined under a binocular microscope and the percent shear noted for some of the specimens (Table 8). Percent shear is the percent of specimen width which failed in shear rather than in brittle fracture. Percent shear is measured on the fracture surface a short distance away from the notch radius to avoid any possible edge effects. It indicates the amount of brittle fracture which occurred. Note

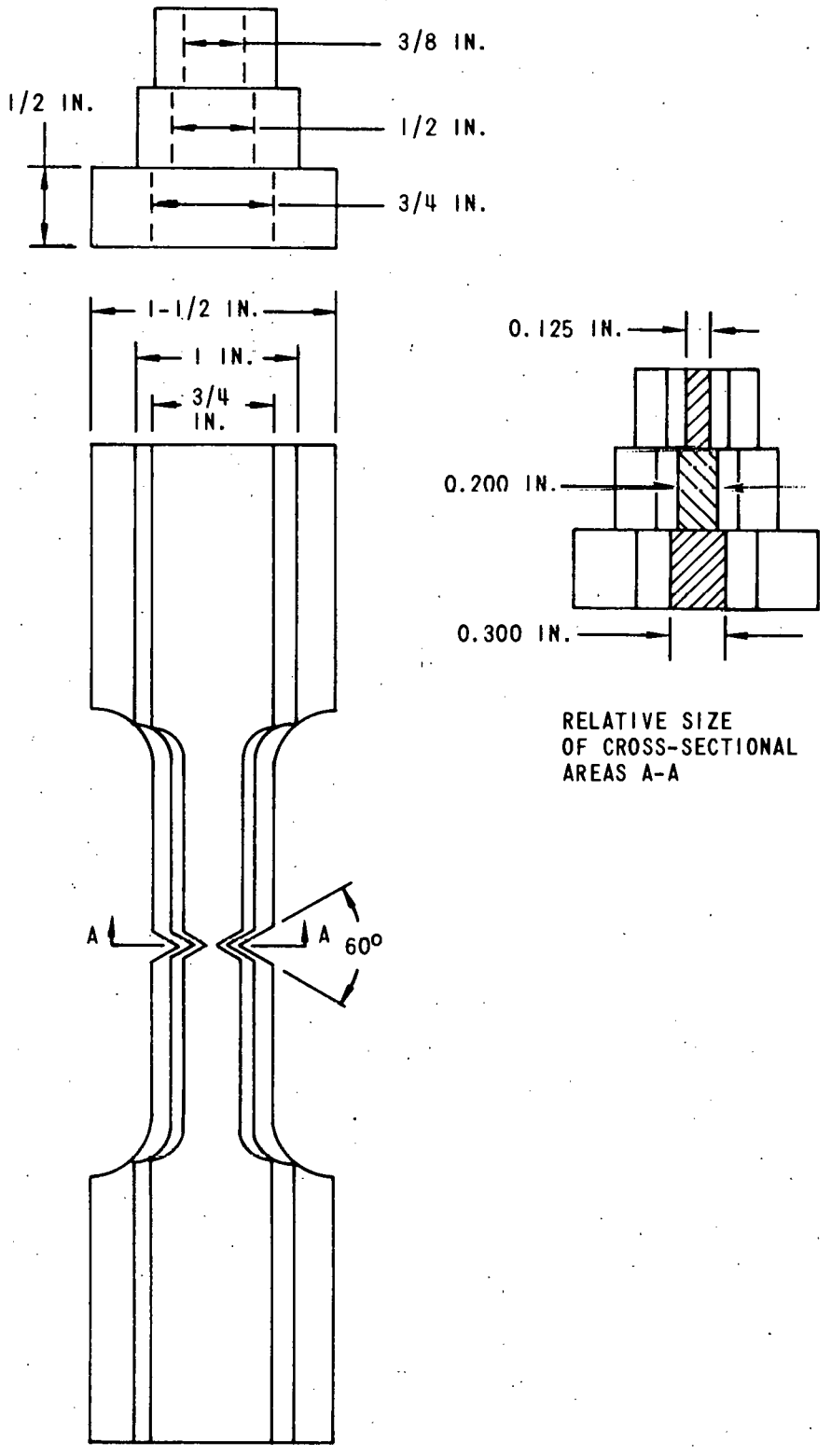

Figure 13. Relative Sizes of Specimens: Series 4

Table 8. Fracture Toughness Test Series 5: Lexan 141, Extruded Sheet Not Annealed

Specimen	Crosshead Speed (ipm)	Fracture Load (lb)	Shear (Percent)	K_{Ic} (psi $\sqrt{in.}$)	K_{Ic} Corrected (psi $\sqrt{in.}$)	Critical Crack Length (in.)
A-1	0.05	600	*	1,503	1,512	0.026
A-2	0.05	1,280	5	3,206	3,307	0.123
A-3	0.05	570	0	1 428	1,437	0.023
A-4	0.05	680	*	1,703	1,847	0.039
A-5	0.5	560	0	1,403	1,412	0.021
B-1	0.05	565	5	1,733	1,756	0.035
B-2	0.05	510	10	1,564	1,581	0.028
B-3	0.05	810	10	2,485	2,549	0.074
B-4	0.05	490	10	1,503	1,519	0.026
B-5	0.05	575	10	1,764	1,787	0.036
C-1	0.05	445	5	1,690	1,874	0.040
C-2	0.05	345	0	1,310	1,441	0.024
C-3	0.4	345	*	1,304	1,441	0.024
C-4	0.4	550	*	1,905	2,323	0.061
C-5	0.5	620	10	2,350	2,648	0.079

* Specimen unavailable

that, on all specimens examined, the percent shear was 10 percent or less, indicating that a good brittle fracture was obtained. As the percent shear drops, K_{Ic} also drops.

A typical load-strain curve presented in Figure 14 shows that the sudden curvature just before fracture shown in Figure 11 has been eliminated. However, there are two slopes to the curve.

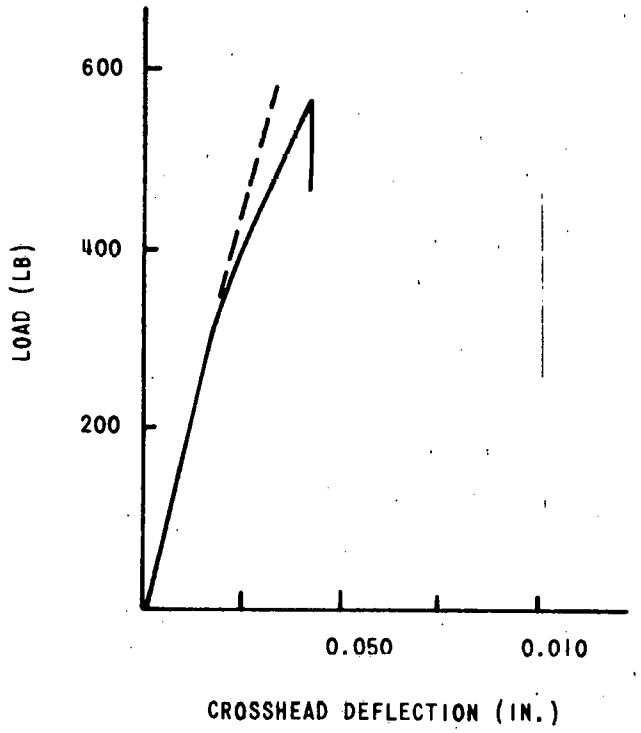

Figure 14. Load-Deflection Curve of Specimen A-3

It was thought at first that these slopes resulted from initial sub-critical crack growth. However, the time span of 0.4 minute to failure was too slow, (see later discussion on high speed movies of a later test). The load level indicated a possible, gradual yielding of the specimen around the notch area.

It is doubtful that complete inelastic fracture is obtained in any engineering material[19] although even rubber appears to tear inelastically at the crack tip.[20] If the yield strength of a material is less than E/10, where E is the elastic modulus, the crack cannot advance elastically and fracture is plastically introduced. This is true of most engineering materials. However these materials can be related to fracture toughness as long as their plastic properties are considered.

To learn the extent of brittle fracture which can occur in polycarbonate, the fracture surfaces of the specimens were examined. Figure 15 shows one surface of Specimen A-3. Tetelman shows this pattern to be a typically normal fracture surface.[22] The fracture surface of A-3 is described in Figure 16. Note that there are three fracture zones: mirror, transition, and rough. The mirror (shiny) surface appears divided into two areas. The dividing line was examined at 100X under reflected light on a metallograph, and found to be seven separate lines which have been called circumferential hesitation lines.[23] They occur when a fast moving crack temporarily stalls and additional stress relaxation takes place.

Although the point of initial fracture is pointed out, it is possible that fracture initiated at several points in this local area and that the fractures joined together to form a main crack front since this occurs readily in highly stressed bodies near failure from uniaxial tension.[24] The ductile "tongue" was caused by a local defect. Note how it affected the crack front in that area (marked by a dimple in the transition zone). Brittle fracture was accelerated locally. It was discovered that the mirror (shiny) region is subcritical crack growth, even though the crack is propagating rapidly. Under a rising tensile load, subcritical cracks grow through plastic deformation which is a small plastic flow zone at the crack tip until the critical crack length is reached. At this point, unstable crack propagation occurs by the release of elastic strain energy. The important flaw or critical crack size is the one which occurs just before subcritical crack growth starts, that is, the original notch depth.[25]

If a crack begins to propagate unstably, the stress field around the crack tip becomes so high that cracks are initiated at flaws ahead of the main crack front. These secondary cracks usually are not in the same plane as the main crack; therefore, tear lines develop where they link. Generally the main crack front will be traveling at a limiting velocity, about 1/3 the sonic velocity of the material, but faster than the velocity of the secondary crack. This action results in characteristic markings such as elongated, parabolic marks on the fracture surface. Examination of several specimens at 100X revealed parabolas of this type (Specimen A-3, Figure 15). A graphic layout of the relative speeds of two crack fronts for one parabola indicated that the main crack front was traveling approximately four times the speed of the secondary crack front. In Figures 15 and 16 the branched lines in the rough region just above the transition zone are called "river markings," and are the result of a secondary cleavage plane.[26]

The observations made thus far clearly establish that critical crack propagation starts at the transition zone, even though the hesitation lines show that a fast moving crack front already existed. From the observations, it is recommended that the specimen fractures be classified as brittle. Other investigators such as Tetelman and McEvily, have also classified polycarbonate fracture toughness specimen fracture surfaces as brittle. It was

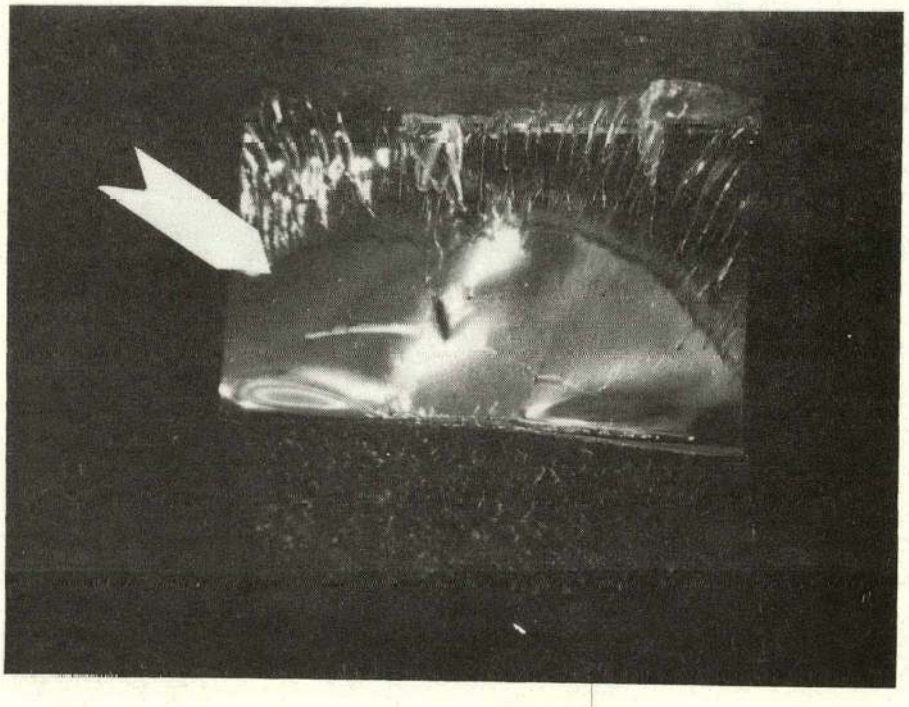

Figure 15. Brittle Fracture Surface of Fracture Toughness Tensile Specimen A-3: Arrow Shows Location of Area Photographed in Figure 17 (4X)

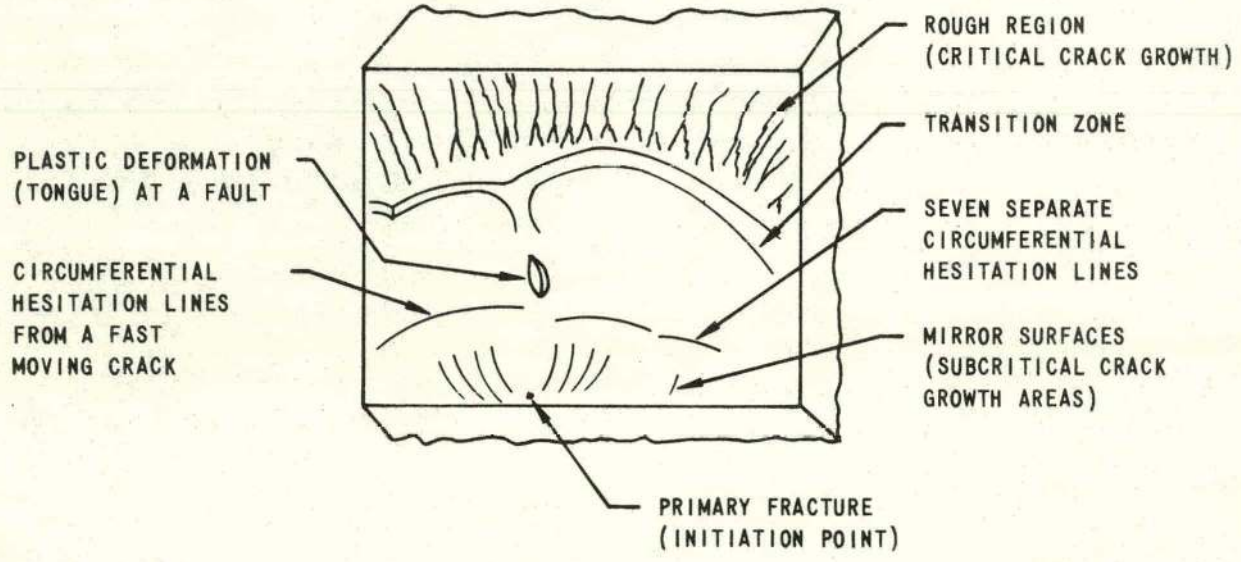

Figure 16. Morphological Pattern of Fracture Surface Shown in Figure 15: Note the Great Similarity of Fracture Features Compared to the Round Specimen in Figure 23

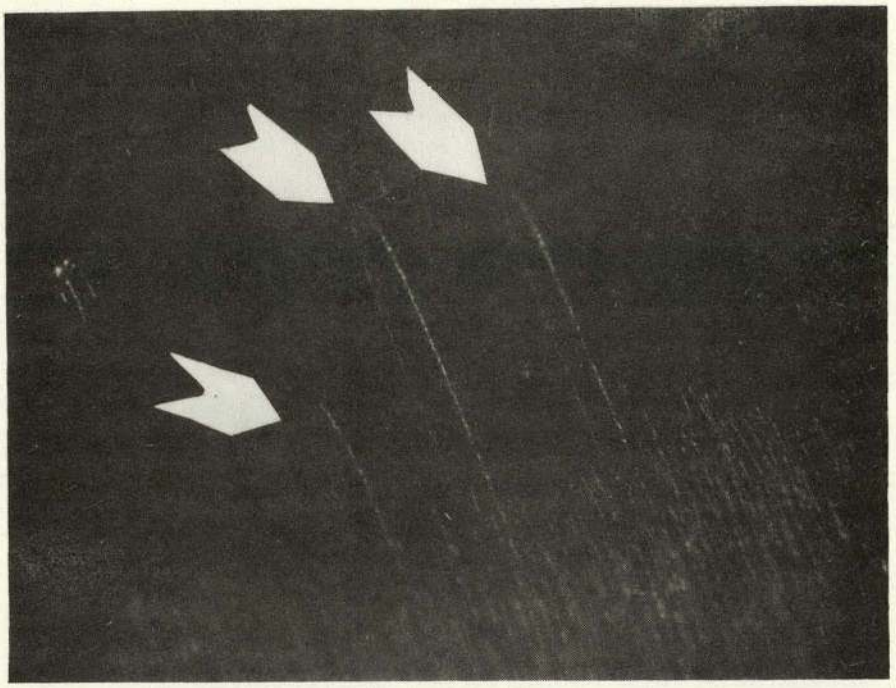

Figure 17. Three Primary and Secondary Crack Front Intersections of Specimen A-3: Elongated Parabolas Show Primary Crack Propagation Front Velocity to be Several Times that of Secondary Fronts. Primary Front Propagated From Top to Bottom. Area Photographed Is Marked by Arrow in Figure 15 (100X)

necessary, however, to reestablish this classification, because test results showed considerable scatter (Figures 18 and 19). Data on the scatter of test results on polymers is not obtainable at present. Scatter on most engineering materials is considerable, which may be the result of geometry (thickness, width, notch, radius), and processing (casting, rolling, forging, welding), as well as temperature level.

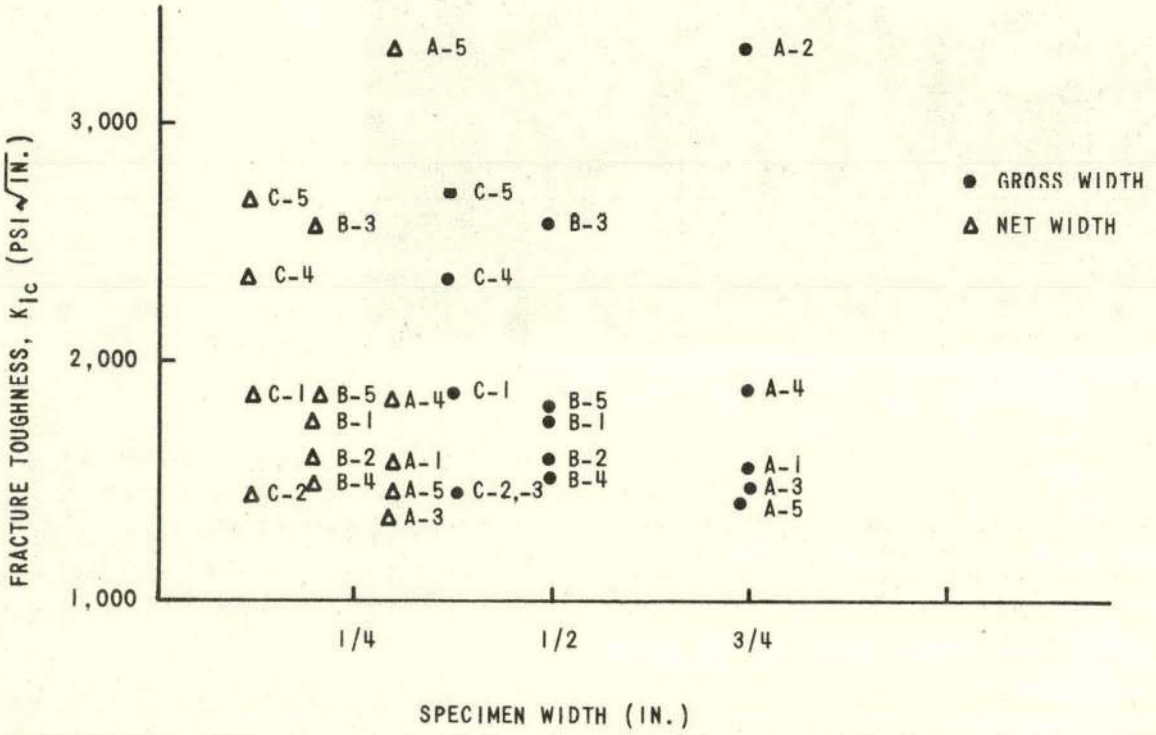

Figure 18. Effect of Specimen Width on Fracture Toughness K_{Ic}: Test Series 5

Note that the critical crack lengths predicted in Table 8 are still valid even though the subcritical crack was larger at failure. A crack at the predicted length will still propagate, whether subcritical or critical, and cause failure. The predicted crack length is still the one at which crack growth starts even though it undergoes some subcritical growth during a rising tensile load.

Rolled Extruded Rod Material

Specimens were designed and tested in Series 4, using extruded, rolled, unannealed rod (Figure 20). The purpose was to learn the effect of bulk geometry (round specimen) and processing (rolling of the rod) upon the rod specimen. The test speed was 0.050 ipm; the results are shown in Table 9.

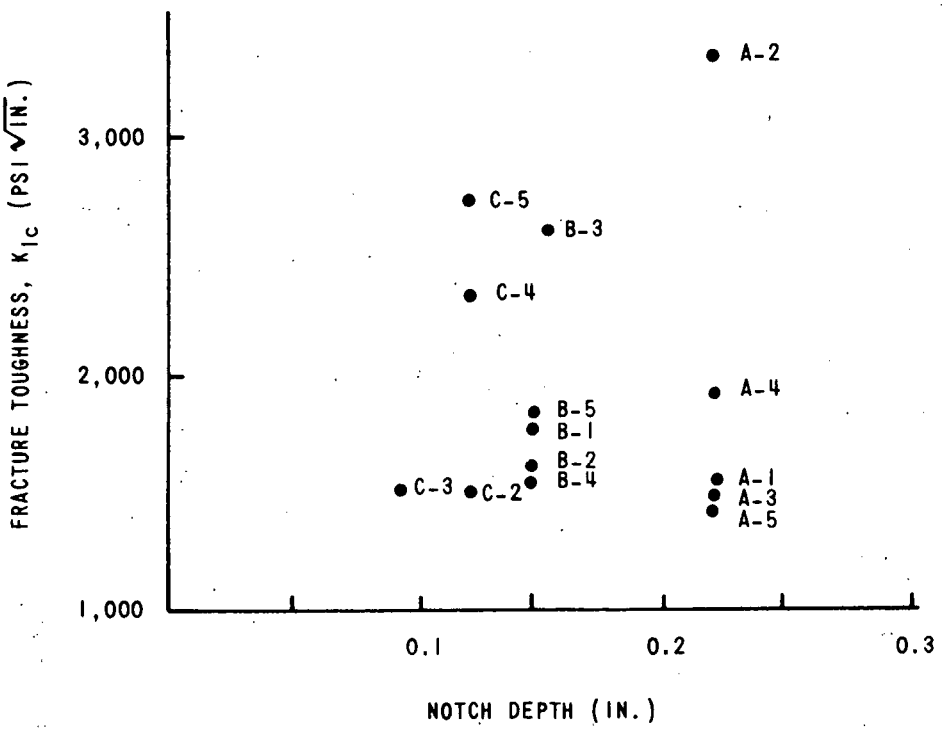

Figure 19. Effect of Notch Depth on Fracture Toughness K_{Ic}: Test Series 5

Table 9. Fracture Toughness Test Series 4: Lexan 141, Rolled Extruded Rod

Specimen	Outside Diameter (in.)	Notch Depth (in.)	Fracture Load (lb)	Shear (Percent)	Fracture Toughness K_{Ic} (psi $\sqrt{in.}$)	Critical Crack Length (in.)
U1	0.50	0.120	650	0	4,050	0.185
U2	0.50	0.120	640	5	3,988	0.180
T1	0.75	1.180	1,230	0	4,169	0.197
T2	0.75	0.180	1,260	0	4,271	0.207
S1	0.875	0.210	1,270	0	3,182	0.114
S2	0.875	0.210	1,210	0	3,032	0.104
L1	0.95	0.240	1,480	0	3,196	0.115
L2	0.95	0.240	1,435	0	3,099	0.109

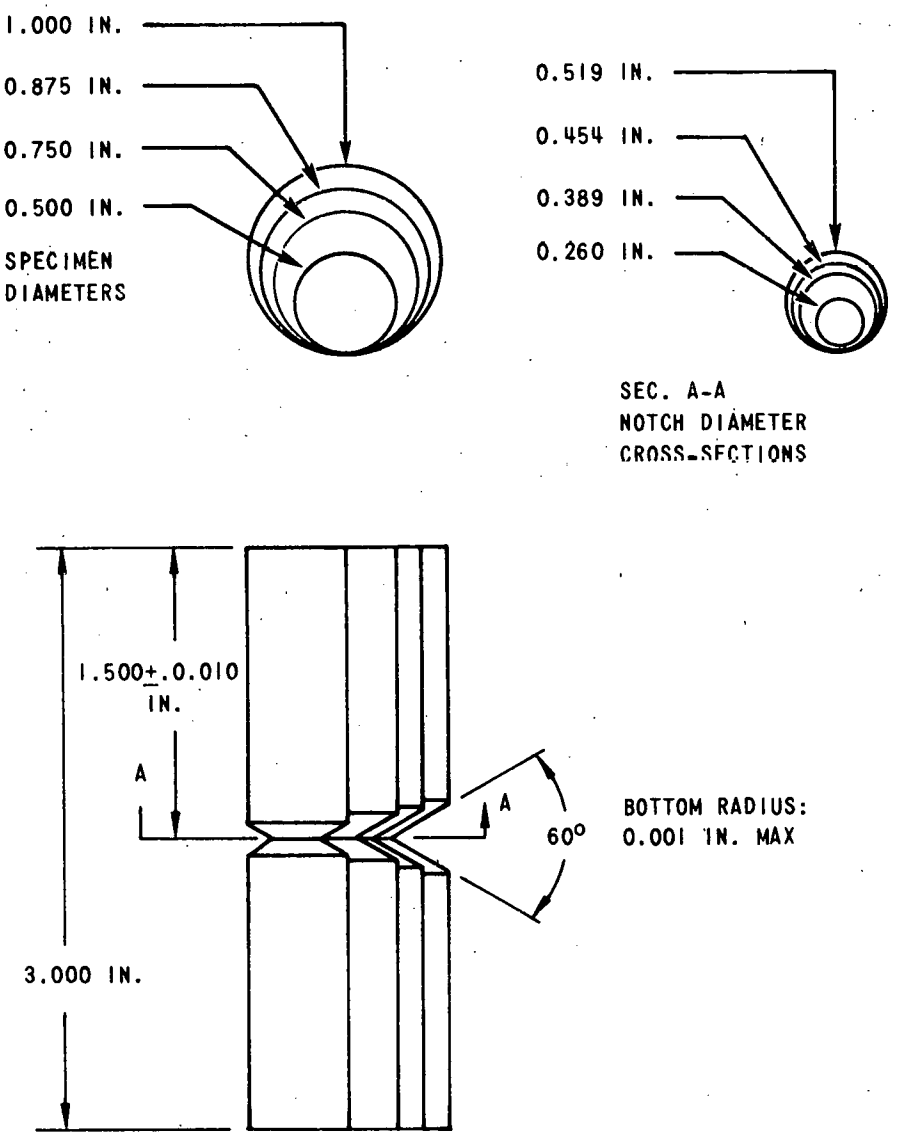

Figure 20. Fracture Toughness: Round Specimens

Fracture Toughness, K_{Ic}, was calculated using Bueckner's formula:[27]

$$K_{Ic} = Y \frac{P}{D^{3/2}}$$

where

K_{Ic} = Plane strain fracture toughness;

Y = Constant (depends on the ratio of the maximum and minimum diameter);

P = Load (lb); and

D = Outside (gross) diameter (in.).

Note that the symbol K_{Ic} is being used in most formulations as long as plane strain fracture predominates. Fracture toughness values are considerably higher for the round specimens than for the flat specimens (Table 8).

Since fracture surfaces appear to be so brittle (Percent Shear, Table 9), K_{Ic} was not corrected with a plastic compliance factor. Critical crack length was calculated using Irwin's formula and a stress level of 5300 psi. Predicted critical crack lengths range from 0.109 to 0.207 inch compared to 0.021 to 0.123 inch for Test Series 5. Since the predicted amount was considerably higher, specimen fracture surfaces were examined. Figure 22 shows one fracture surface of specimen L1, and Figure 23 points out the surface features. This was a typically normal brittle fracture very similar to that obtained by other investigators such as Tetelman and McEvily. The transition zone is larger on round specimens and tear lines are radial. Ductile fracture striations appeared for the first time. These appear to be Wallner's lines which are often found in metals.[28] They occur when an advancing crack front interacts with an elastic wave propagating at the same time. They occur in very brittle fracture. A compression net about 0.030- to 0.040-inch deep appears around the entire edge and indicates that high residual stresses were locked into the material during machining and when rolled into a rod. This processing or rolling may have raised the fracture toughness values shown in Table 9 either through residual stresses, elimination of tiny defects or voids, smoothing of surface finish, or realignment of residual stress direction (rolling was at an angle of 30° to the axis).

Figure 21 shows the effect of the maximum or gross specimen diameter on fracture toughness, K_{Ic}. There appears to be a transition point between the 3/4- and 7/8-inch diameters where the fracture toughness decreases considerably. This transition point may be a bulk effect and may indicate that round K_{Ic} specimens should be larger than 3/4 inch in diameter.

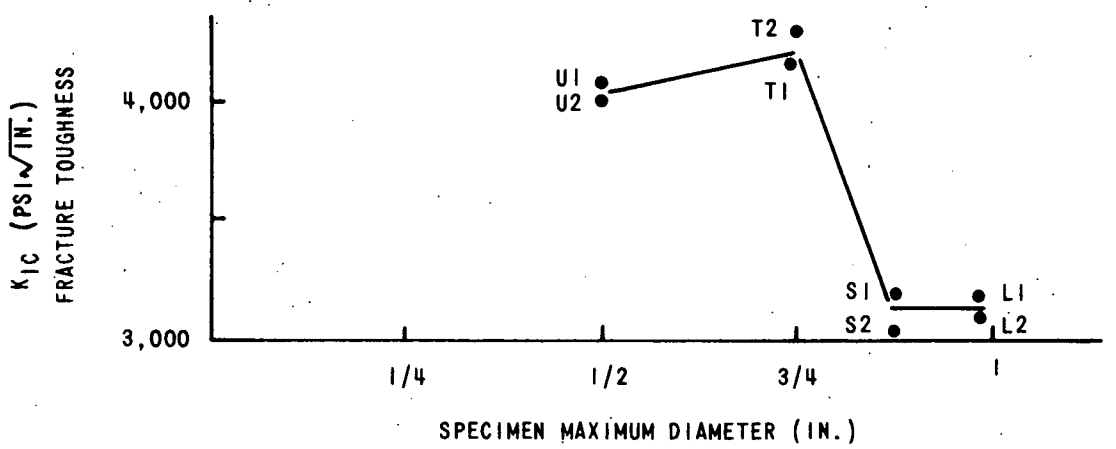

Figure 21. Effect of Diameter on Fracture Toughness

As more test evidence is gathered, polycarbonate proves to be a normally ductile material which can behave as a brittle material in biaxial stress and plane strain conditions. Since this behavior is an anomaly, an independent check on the ductility of the material was made by calculating the notch-sensitivity ratio of the fracture toughness specimens (Table 10).

The calculation used in the following formula is:

$$N = \frac{\sigma net}{\sigma ultimate}$$

where:

N = Notch-sensitivity ratio;

σ net = Fracture stress on minimum (net) area at the notch (psi); and

σ ultimate = Ultimate stress of the material (psi).

The notch-sensitivity ratio of a material is a measure of the ability of a material to resist stress concentration. If a material is not notch-sensitive, the ratio will be one. If a material is notch-sensitive it will be affected by stress concentration, and the ratio will be less than one. Surprisingly, a ductile material can have a ratio greater than one; that is, the stress at fracture is greater than the ultimate strength. This is possible for a tensile test since the notch constrains the material locally (called elastic or plastic constraint by Tetelman) and fatigue or cycling is not involved.

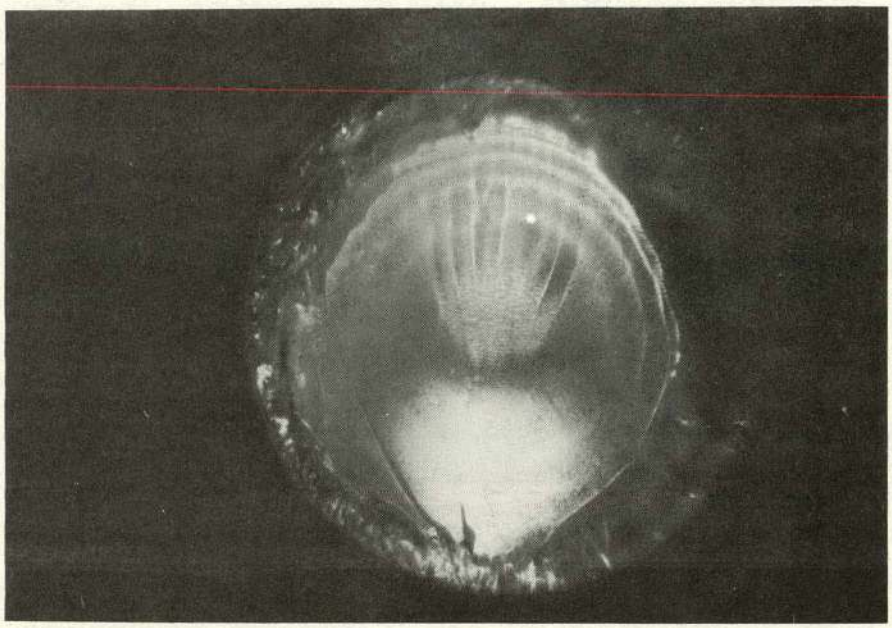

Figure 22. Polycarbonate Brittle Fracture Surface of 0.950-Inch-Diameter Tensile Specimen L-1 With 0.225-Inch-Deep Notch and 0.001-Inch Maximum Root Radius (4X)

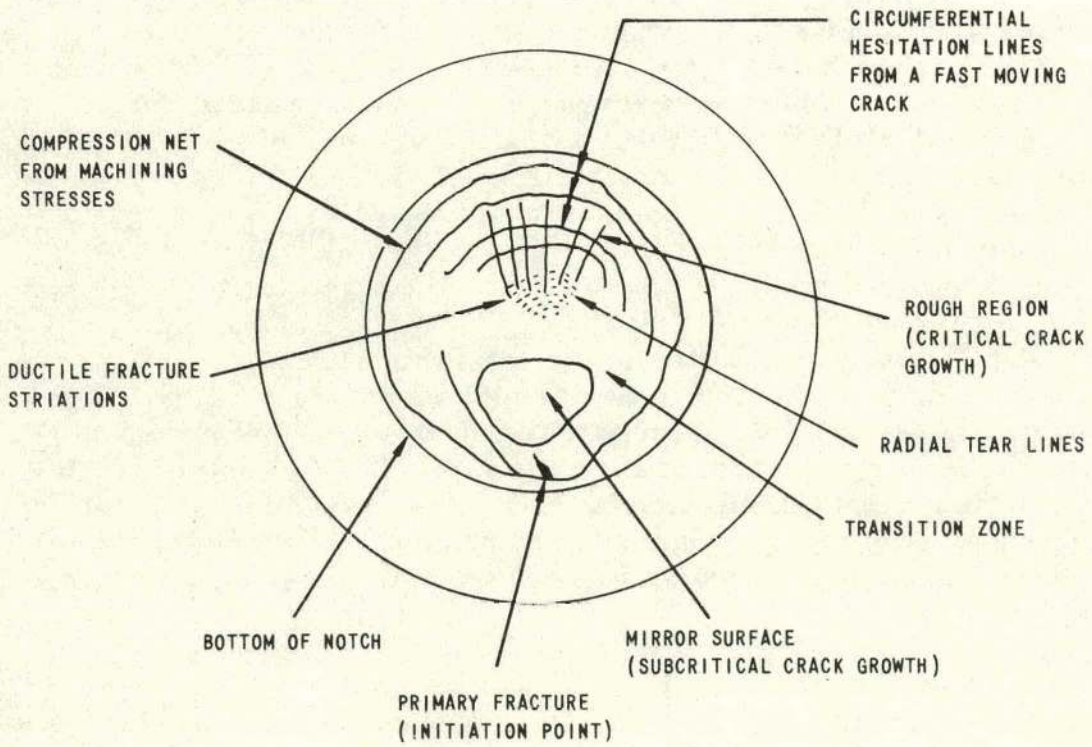

Figure 23. Morphological Pattern of the Fracture Surface Shown in Figure 22: a Normal Non-Metallic Brittle Fracture Is Shown

Table 10. Notch-Sensitivity Ratios for Fracture Toughness Specimens

Specimen	Test Series					
	2	3	4	5A	5B	5C
1	0.93	1.08	1.18	0.38	0.54	0.76
2	0.93	0.919	1.21	0.41	0.49	0.59
3	0.93	0.82	1.40	0.36	0.78	0.59
4	0.95	0.86	1.37	0.43	0.47	0.93
5	0.96	0.94	0.77	0.36	0.55	1.05
6	0.94	1.05	0.73			
7	0.94		0.96			
8			0.93			

Table 10 shows that under some conditions (in 7 specimens or 19 percent) polycarbonate is not notch-sensitive. However, in 81 percent of the specimens there was a notch effect, which was severe in 15 specimens (41 percent). In 7 cases (19 percent) the strength was reduced by more than half. Other investigators have found that if the notch sensitivity ratio is less than 0.70, there is strong probability that an unstable fracture or crack propagation will occur in service. Therefore, study of fracture toughness and stress-cracks in polycarbonate should continue.

Since there was considerable scatter in the data when it was plotted without regard to processing or geometry, a scalar plot was made of all fracture toughness test data (Figure 24). It appears from this plot that processing affects data as much as, if not more than, geometry. Apparently fracture toughness of polycarbonate is affected by most of the variables which affect fracture toughness of metals. Fracture toughness values should be determined for each basic material process as is now done for metal preparation.

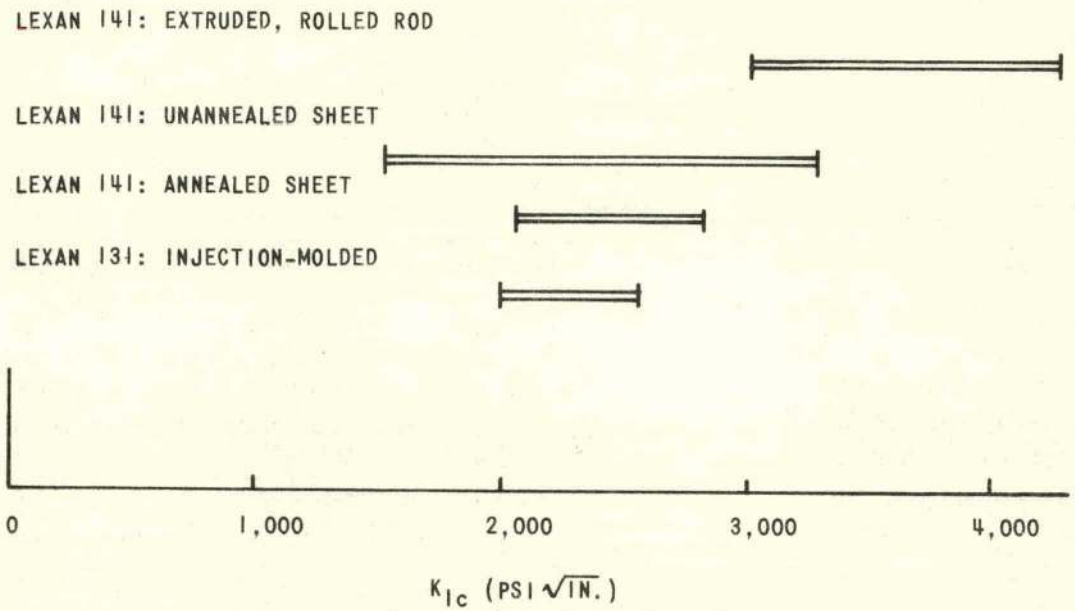

Figure 24. Effects of Processing, K_{Ic}, and Geometry on Fracture Toughness

Plastic Compliance Factor

Although local defects can affect stress-cracking, processing and geometry more generally lessen the basic ability of the material to resist stress-cracking. These factors, in turn, should greatly affect the size and shape of the plastic flow zone at the edge of a stress-crack or at the tip of a propagating crack front. Because the size of the plastic flow zone determines the ability of a material to resist stress-cracking and crack propagation, the actual size of the plastic flow zone was measured rather than theoretically corrected as a plastic compliance factor to predict more accurately significant stress-crack sizes.

Another group of notched tensile specimens was designed, as shown in Figure 25 and Table 11, in which the thickness, width, notch depth, and root radius are varied. Previous specimen design was based on available engineering information from the literature. Because of the many variables, it is now desirable to use a statistically designed experiment to determine if variables are significant and to cover a large enough range. The thickness of tested specimens has been thinner than some investigators prefer when establishing minimum fracture toughness values. The thickness of these specimens, however, provides more representative fracture toughness values for immediate use. A $(two)^4$ factorial analysis, shown in the four factors at two levels in Table 12, resulted in 16 different specimens. Two specimens of each kind were machined from a General Electric non-annealed, half-inch extruded sheet.

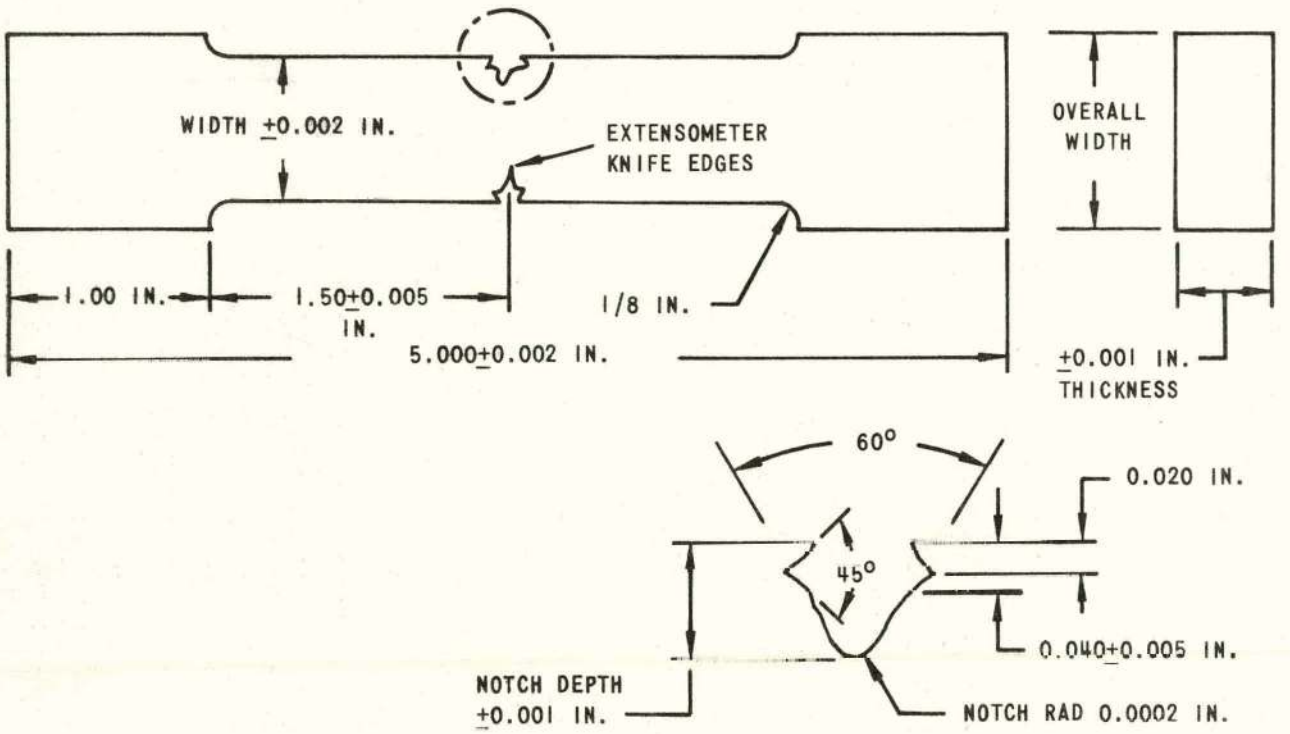

Figure 25. Typical Plastic Compliance Factor Specimen

Table 11. Design Variables for Plastic Compliance Specimens: Test Series 6

Specimen	Width (in.)	Thickness (in.)	Overall Width (in.)	Notch Depth (in.)	Notch Radius (in.)
ABCD	0.750	0.490	1.00	0.150	0.010
ABC	0.750	0.490	1.00	0.150	0.002
ABD	0.750	0.490	1.00	0.075	0.010
AB	0.750	0.490	1.00	0.075	0.002
CD	0.375	0.250	0.750	0.150	0.010
C	0.375	0.250	0.750	0.150	0.002
D	0.375	0.250	0.750	0.075	0.010
(1)	0.375	0.250	0.750	0.075	0.002
ACD	0.750	0.250	1.000	0.150	0.010
AC	0.750	0.250	1.000	0.150	0.002
AD	0.750	0.250	1.000	0.075	0.010
A	0.750	0.250	1.000	0.075	0.002
BCD	0.375	0.490	0.750	0.150	0.010
BC	0.375	0.490	0.750	0.150	0.002
BD	0.375	0.490	0.750	0.075	0.010
B	0.375	0.490	0.750	0.075	0.002

Until now, only crosshead strain was recorded since the hard, smooth specimen surface was difficult to grasp. Since the plastic flow area is now being studied, a better indication of strain in the notch is needed. (Note that at all times the notch simulates a crack length which is equal to the notch depth.) A special strain gage extensometer, shown in Figure 26, was built of a 0.032-inch-thick aluminum strip 0.250 inch wide, and an overall gage length of 2 inches. A foil strain gage was bonded to the outside of the bend with polymide EPY-600. A 1/64-inch radius was machined into each end of the extensometer. The ends grasp the small knife edges machined into the notch on each specimen. The spring action of the extensometer holds it on the specimen. The extensometer was calibrated with an existing Tucson micrometer head mounted in a Bendix-designed base.

Table 12. Plastic Compliance Factor Experiment Design

Symbol	Variable	Level 1 (in.)	Level 2 (in.)
A	Width	0.375	0.75
B	Thickness	0.25	0.49
C	Notch Depth	0.075	0.150
D	Notch Radius	0.002	0.010

Testing was conducted at a crosshead speed of 0.5 ipm on a 10,000 pound Instron tensile tester. A typically flat fracture was obtained on all specimens. Since there was a considerable amount of test data, a small Fortran IV computer program (Appendix B) was written and the data was reduced on an IBM 360. Sample printouts, Items 1, 2, and 3, in the computer program description present the results as printed out by the computer. Item 3 indicates that significant parameters at the 95-percent confidence level are specimen width and notch depth, and that there is an interaction between them. This fact is borne out by Bowie who showed theoretically that notch width and notch depth affect fracture toughness non-linearly.[29] Thickness and notch radius proved insignificant, which is contrary to all expectations.

Table 13 presents all specimens tested in this series. Since two specimens of each design were tested, they are labeled (-1) and (-2). The fracture toughness values vary slightly from those shown in Appendix B because they were calculated from actual cross-sectional areas, whereas nominal values were used on the computer. Fracture stress or net notch stress is shown, in addition to the plastic zone compliance factor. This factor was 12 percent

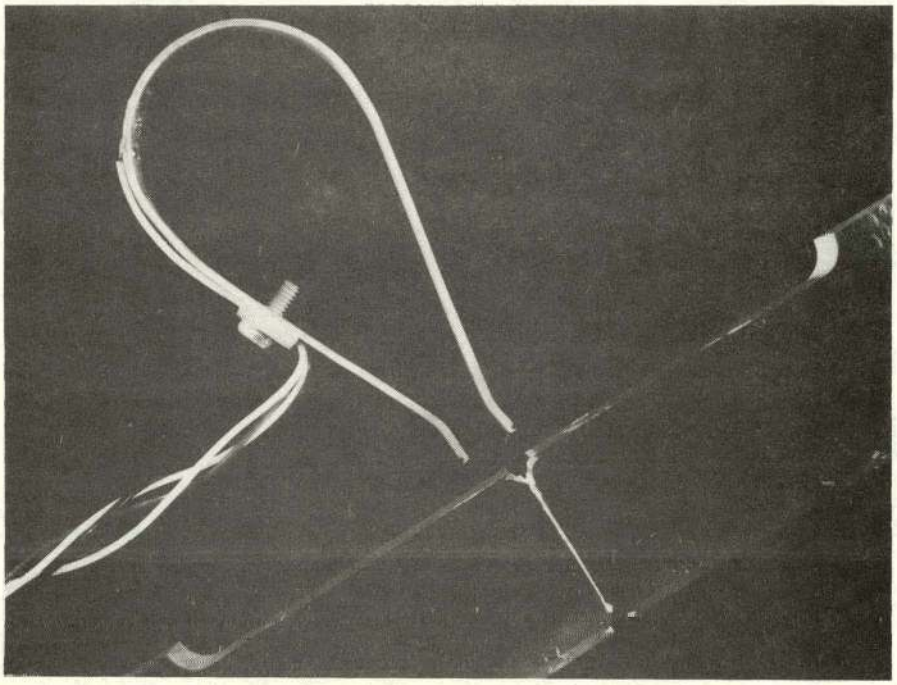

Figure 26. Typical Fractured Specimen and Strain Gage Extensometer for Measuring Notch Strain

of the predicted crack length for all specimens and was added to the predicted crack lengths shown. Crack lengths were predicted using Irwin's formula for a stress level of 5300 psi since stress-cracks have been found at this stress level.

A 0.070 to 0.232-inch spread of predicted crack lengths was obtained and all crack lengths were considerably larger than expected since notch design was essentially the same as Test Series 4. In addition, there is some difference between the ultimate elongation of each pair of specimens, and it is greater for pairs with the smallest notch radius. Figure 27 shows the huge difference in plastic flow between specimen pair AC-1 and AC-2. In Table 13 note that some specimens failed at net stress levels below the elastic limit.

Since specimen fracture surfaces appeared very brittle to the naked eye, they were examined at 100X with a metallograph using a dark field. It was discovered that fracture in some specimens was initiated in a ductile manner. Figure 28 shows Specimen ABC-2 fractured when a ductile plug of material sheared out in the axial direction. The plug sides are vertical, and the plug itself is approximately 0.006 inch in diameter and 0.002 inch high. It is

Table 13. Test Results of Plastic Compliance Factors

Specimen	Width (in.)	Thickness (in.)	Notch Depth (in.)	Notch Radius (in.)	Ultimate Elongation (in.)	Net Fracture Stress (psi)	Fracture Toughness K_I (psi $\sqrt{in.}$)	Plastic Zone Compliance Factor (in.)	Predicted Crack Length (in.)
ABCD-1	0.75	0.49	0.150	0.010	0.014	7,737	3,636	0.019	0.168
ABCD-2	0.75	0.49	0.150	0.010	0.015	7,737	3,630	0.019	0.168
ABC-1	0.75	0.49	0.150	0.002	0.013	7,354	3,465	0.018	0.154
ABC-2	0.75	0.49	0.150	0.002	0.011	7,264	3,423	0.017	0.149
ABD-1	0.75	0.49	0.075	0.010	0.012	7,653	3,312	0.016	0.141
ABD-2	0.75	0.49	0.075	0.010	0.017	7,908	3,446	0.018	0.151
AB-1	0.75	0.49	0.075	0.002	0.016	8,247	3,615	0.019	0.166
AB-2	0.75	0.49	0.075	0.002	0.010	6,959	3,050	0.014	0.119
CD-1	0.375	0.25	0.150	0.010	0.014	9,473	1,937	0.006	0.049
CD-2	0.375	0.025	0.150	0.010	0.013	11,947	2,443	0.009	0.077
C-1	0.375	0.025	0.150	0.002	0.018	11,500	2,467	0.009	0.077
C-2	0.375	0.025	0.150	0.002	0.012	11,650	2,495	0.009	0.077
D-1	0.375	0.25	0.075	0.010	0.014	9,325	2,977	0.010	0.100
D-2	0.375	0.25	0.075	0.010	0.012	10,086	3,321	0.016	0.141
(1)-1	0.375	0.25	0.075	0.002	0.018	8,169	2,717	0.011	0.094
(1)-2	0.375	0.25	0.075	0.002	0.010	9,067	3,016	0.013	0.116
ACD-1	0.75	0.25	0.150	0.010	0.014	6,637	3,070	0.015	0.122
ACD-2	0.75	0.25	0.150	0.010	0.011	6,902	3,193	0.015	0.130
AC-1	0.75	0.25	0.150	0.002	0.061	7,964	3,696	0.021	0.175
AC-2	0.75	0.25	0.150	0.002	0.014	9,203	4,272	0.027	0.232
AD-1	0.75	0.25	0.075	0.010	0.077	9,066	3,983	0.023	0.202
AD-2	0.75	0.25	0.075	0.010	0.081	8,333	3,661	0.020	0.170
A-1	0.75	0.25	0.075	0.002	0.020	7,733	3,386	0.017	0.147
A-2	0.75	0.25	0.075	0.002	0.014	8,200	3,590	0.019	0.164
BCD-1	0.375	0.49	0.150	0.010	0.010	10,285	2,013	0.006	0.051
BCD-2	0.375	0.49	0.150	0.010	0.008	10,857	2,125	0.007	0.058
BC-1	0.375	0.49	0.150	0.002	0.011	10,750	2,369	0.008	0.070
BC-2	0.375	0.49	0.150	0.002	0.010	12,125	2,672	0.011	0.092
BD-1	0.375	0.49	0.075	0.010	0.011	9,035	3,000	0.013	0.115
BD-2	0.375	0.49	0.075	0.010	0.011	9,429	3,131	0.015	0.126
B-1	0.375	0.49	0.075	0.002	0.017	7,916	3,320	0.016	0.140
B-2	0.375	0.49	0.075	0.002	0.009	6,805	2,854	0.012	0.104

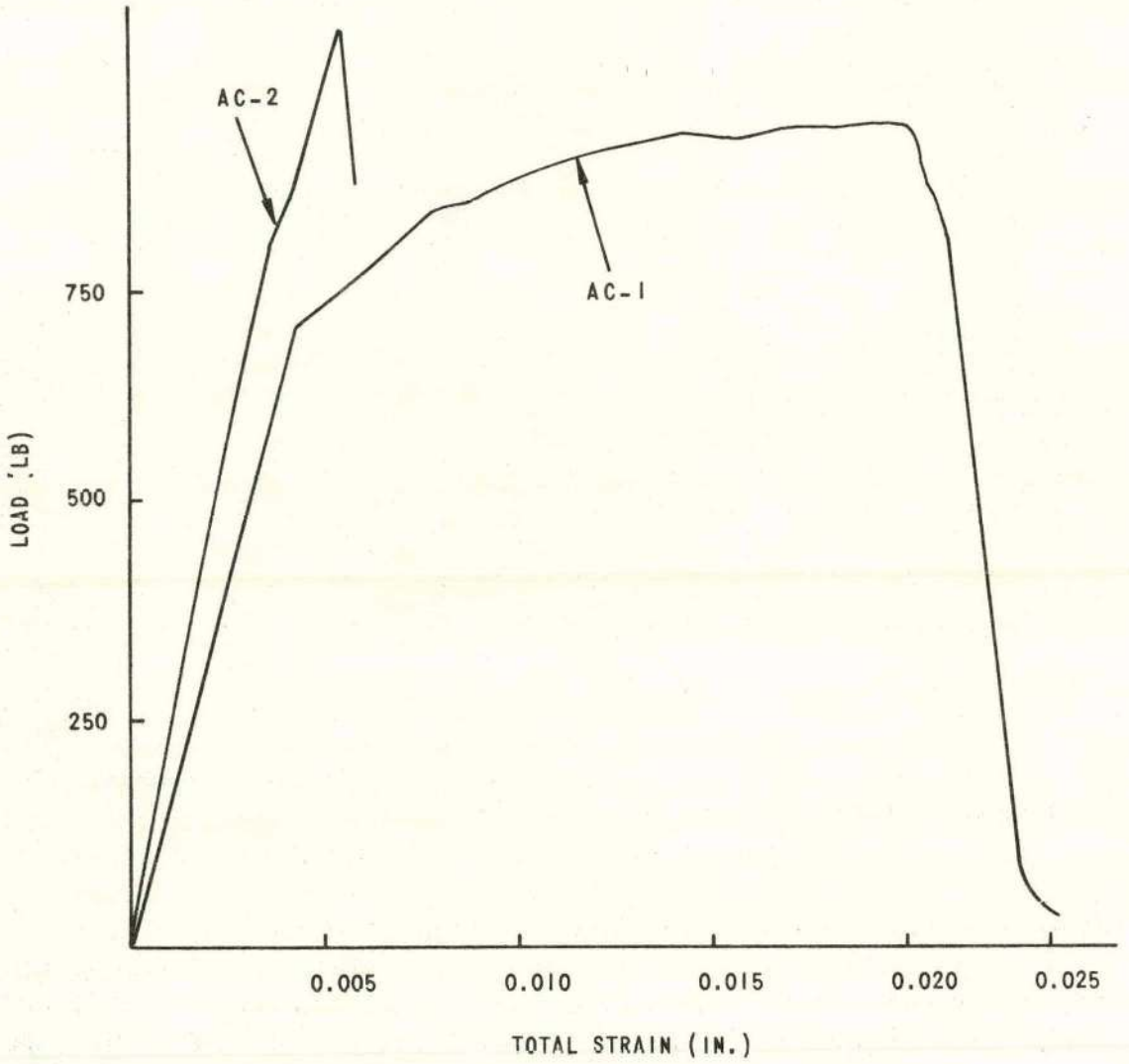

Figure 27. Variation in Plastic Flow in the Notch Between Specimens AC-1 and AC-2

located back of the notch radius several thousandths of an inch, indicating that a fairly large plastic zone developed before fracture. Ductile fracture striations were found on some specimens.

Green and red interference colors were noted in some areas on some fracture surfaces. These colors disappear after several weeks. This effect occurs in other polymers, such as green and purple in polymethyl methacrylate.[30, 31] The material in the colored areas has different molecular orientation and is of a different density than the parent material, indicating that strain energy is the cause of this effect. This is a surface effect and affects only a thin layer of the material. The colors apparently result from fracture occurring

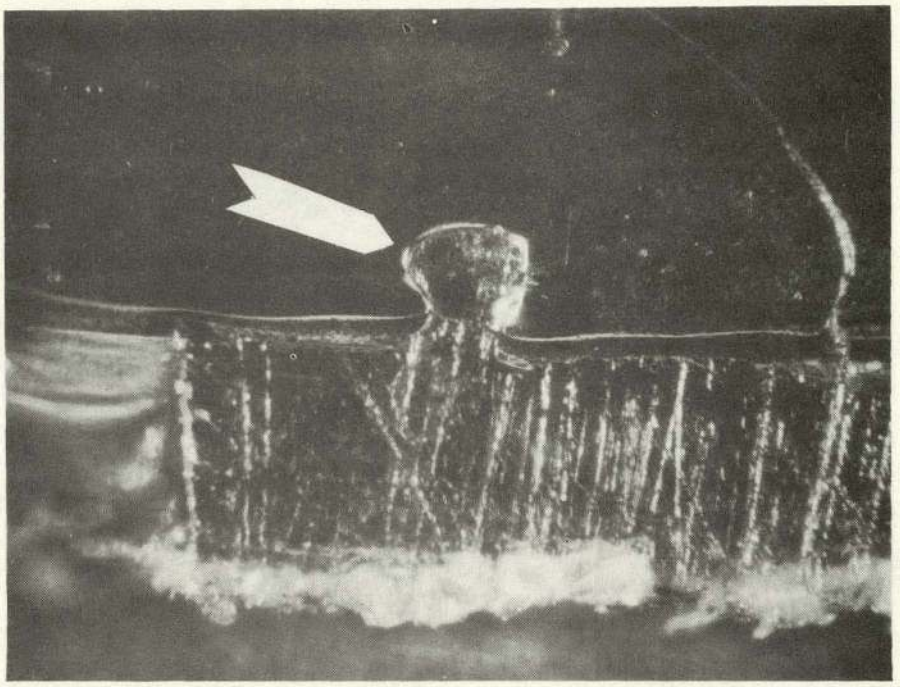

Figure 28. Fracture Surface of Plastic Compliance Specimen ABC-2 Showing Point of Fracture Initiation (Arrow) Which Occurred Ductilely by Tensile Shear. Initial Failure Is Raised Material Below Notch Surface and Ahead of Simulated Crack (100X)

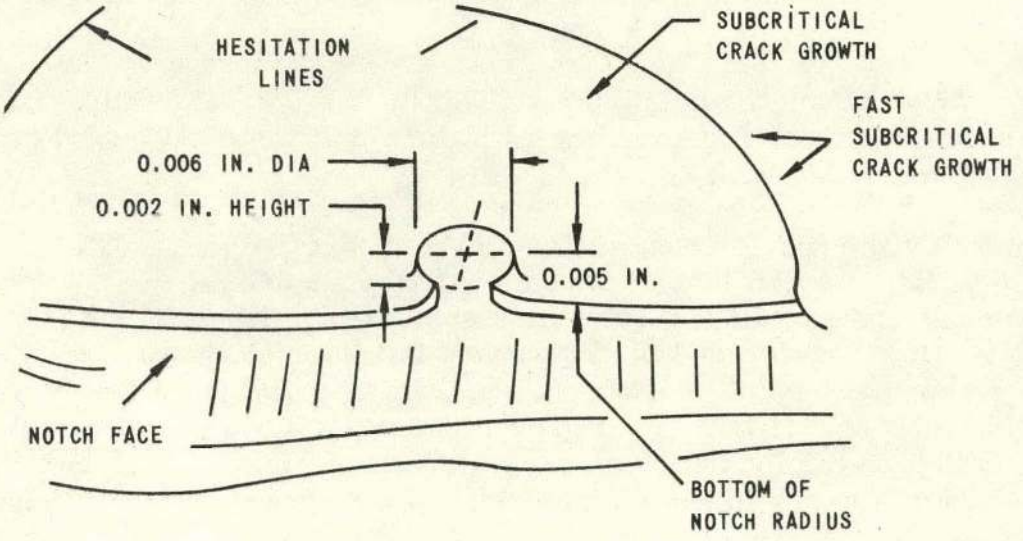

Figure 29. Surface Features of Specimen ABC-2 Shown in Figure 28

on two closely-spaced parallel planes. The crack alternates from one plane to the other. The height difference between the planes produces the color interference effect. This phenomenon is a viscous flow, dissipative process and disappears as the crack velocity increases. Because of the small volume, only a tiny amount of strain energy is used to create this effect, and consequently, the resulting error is small.[32] This color effect usually starts at a flaw and the structure of this thin layer resembles that of craze marks. Parabolas caused by secondary cracks were found farther along the path of the crack, indicating that crack propagation was rapid. Therefore, it appeared that the fracture was brittle but initiated in a ductile manner.

The notch radii of the (-1) specimens were examined and it was found that instead of specimens with two different notch radii of 0.002 and 0.010 inch, there were 11 specimens of 0.002-inch radius, 2 of 0.001-inch, 1 of 0.004-inch, and 2 of 0.010-inch radius. This is one reason the computer analysis yielded no significance in notch radius. It has since been determined that a 0.001-inch-radius maximum is needed to give the lowest possible fracture toughness values, which indicates the range of the notch radius was too high.

Other investigators, such as L. R. Calcote and C. E. Bowman, have measured the size of the plastic flow zone by establishing the elastic-plastic boundary photoelastically. Therefore, color movies were taken of the isochromatic patterns around the notches of seven of the (-2) specimens during testing. As suspected, many fringes were present but too faint to be interpreted. Hence, a helium-neon laser with a 4-milliwatt continuous output was used to provide monochromatic light for the other nine (-2) specimens.

A camera recorded fringe patterns at 50 frames-per-second and Figure 30 shows fringes forming around the notch of a typical specimen. The fringes became so numerous and close together before failure that the elastic-plastic boundary could not be established.

Calculations show that the fringe constant for polycarbonate, which is 33 psi per fringe per inch, is so small that 64 fringes will appear around the notch before plastic flow starts on this 1/4-inch-thick specimen. Hence, future study of the plastic flow zone around the notch may be accomplished more easily using holography, as pointed out by T. D. Dudderar and R. O'Regan. It appeared at first that subcritical crack growth occurred slowly and initiated at a point of inflection on the load-strain curve. However, motion picture photography showed that crack initiation and propagation occurs in a fraction of a second.

This test series shows that determination of the plastic flow zone size is difficult but can eventually be accomplished. It also shows that a very small radius is required to obtain minimum K_{Ic} values. It should be noted, however,

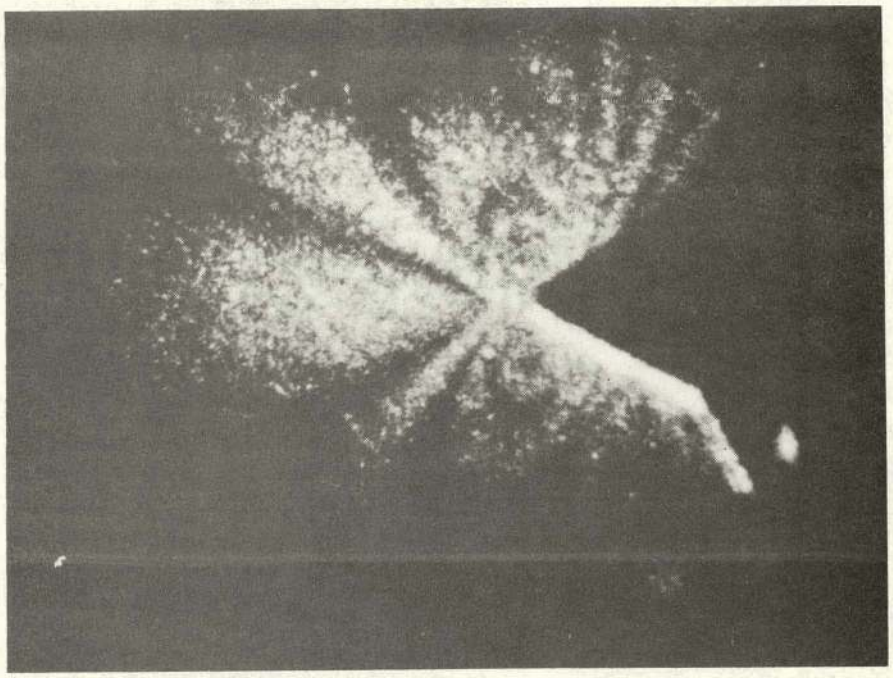

Figure 30. Photoelastic Fringes Around a Notch at Approximately One-Half the Elastic Limit: Specimen ACD-2

that the correction factor for this series was only 11 percent, though some fractures initiated ductility. This percentage probably will be reduced below 5 percent by reducing the notch radius below 0.001 inch.

Future Testing for Fracture Toughness

The fracture toughness of polycarbonate apparently will vary with processing and geometry. However, it is practical to determine these parameters and to predict critical crack lengths for use in engineering, processing, and quality control. It is apparent that fracture toughness should be considered in the designing, manufacturing, and inspection of polycarbonate material. The tremendous elongation (90 to 140 percent) of polycarbonate in tensile testing tends to make stress-cracks appear unimportant. However, some of the unusual characteristics of polycarbonate make stress-cracks and fracture toughness most important factors.

The previous report on this project showed that polycarbonate, despite its ductility, can be sensitive to a difference of 0.002 inch of thickness (1-1/2 percent) in a simple tensile test. Touching a specimen with the human hand will cause the material to fail in that area during a tensile test. Polycarbonate stress-cracks readily under dead-loads as low as 5300 psi, and these

cracks grow larger with time. The fracture toughness of polycarbonate is not as high as would be expected from its tensile elongation. Testing to date indicates that stress-cracks can be significant when they are as small as 0.021 inch in length at a stress level of 5300 psi. At a recommended design stress of 1000 psi, a stress of 5300 psi, which is two-thirds of the yield strength, will be encountered occasionally in local areas. Even shorter cracks will cause failure at higher stresses, which implies that failures may occur in service. Polycarbonate appears to be sensitive to stress concentrations where deflection is limited which can occur in roots of gear teeth, or radii on stepped shoulders. Avoiding these conditions will improve fracture resistance of polycarbonate, but will not eliminate the stress-cracks which arise from local material defects.

The fracture toughness (K_{Ic} values) of Test Series 2, 3, 4, and 5 are considered valid, and it is believed the predicted crack lengths are realistic. The predicted values of Test Series 6 are probably too high. Additional testing is needed to better define when and under what conditions of processing that stress-cracks become critical. For example, injection-molded parts tend to have their surface molecules oriented perpendicularly to the direction of material flow into the mold. This situation can produce a high residual stress in the skin. It is believed that the tensile failure shown in Figure 28 could have been caused by residual machining stresses just below the surface, or by a local defect.

The lowest value of fracture toughness obtained was $K_{Ic} = 1412$ psi $\sqrt{\text{in.}}$ A value of 1140 to 1200 psi was found in the Mukherjee article. However, this range is not comparable with tensile figures since it was obtained by fatigue testing. The range probably represents the lowest limit to be expected for polycarbonate at room temperature. Thicker and wider specimens, however, may reduce the values and should be investigated in this possibility. Testing should also be conducted at low temperature because fracture toughness and critical crack length decrease appreciably at lower temperatures.[33] Amorphous regions of polymers become brittle at low temperatures.

CONCLUSIONS AND RECOMMENDATIONS

Testing to date represents about 30 percent of that believed necessary to characterize stress-cracking of polycarbonate. It is believed that additional testing could produce valuable data, such as that shown in Figure 31, which could be used for process control and quality control. Figure 31 shows the effect of the ligament (net cross-sectional) area on fracture toughness. It also shows that, as the ratio of crack length to specimen width (2a/W) decreases, fracture toughness also decreases. The data for each group of specimens was averaged since there was considerable scatter within the groups. Additional testing should reduce this scatter considerably. Fracture toughness is also reduced by radiation. Its effect on stress-cracking of polycarbonate should also be investigated.

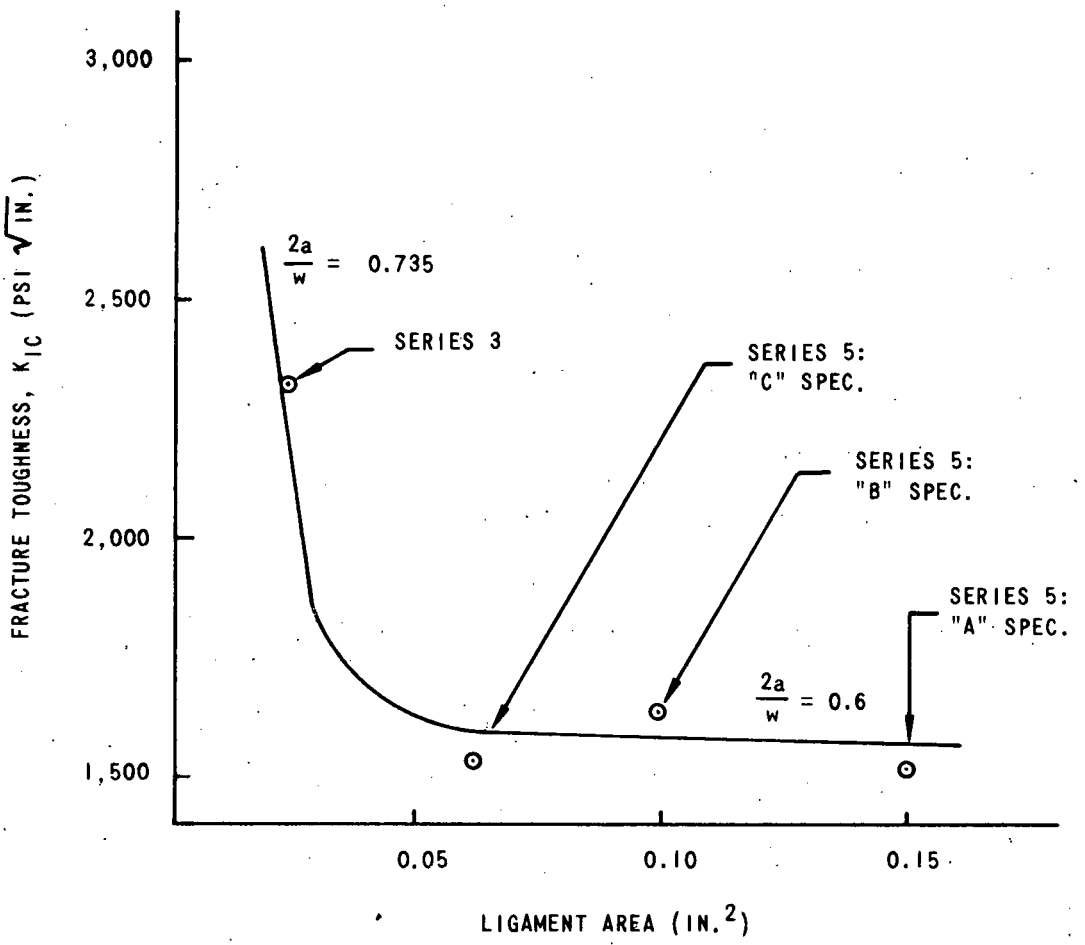

Figure 31. Variation of K_{Ic} With Ligament (Net Cross-Sectional) Area and Crack Length to Specimen Width Ratio (2a/W)

In summary, this investigation on stress-cracking in polycarbonates yields nine conclusions.

- Polycarbonate stress-cracks readily at stress levels well below its yield strength in tensile creep, uniaxial fatigue and biaxial tension.
- High humidity increases susceptibility to stress-cracking.
- Notch sensitivity ratios indicate small stress-cracks may cause failure in polycarbonate parts in service.
- Fracture toughness tests indicate cracks as small as 0.021 inch in length may cause failure of parts in service.

- Residual stresses can be nearly eliminated by a 320°F, 100-hour anneal in argon, although some loss in ductility will be experienced.

- Fracture toughness appears to be an effective criterion for predicting significant stress-crack lengths.

- Stress-cracks greatly reduce the endurance limit of polycarbonate.

- Stress-cracks in polycarbonate are greatly influenced by processing methods and the design factors of geometry and deflection.

- The ductility of polycarbonate appears to prevent stress-cracking in uniaxial tensile tests and impact tests.

Therefore, it is recommended that:

- The dead-load creep tests be continued since it is believed that stress-cracks will eventually cause failure (Additional specimens should be tested at other stress levels to provide a greater range of data);

- Fracture toughness testing be continued using thicker and wider specimens because stress-cracking is more severe under these conditions;

- The effects of stress-cracking on low cycle plastic strain be investigated since many service parts will experience this type of loading; and

- The fracture toughness of other polymers used at Bendix be determined.

Appendix A

FRACTURE TOUGHNESS SYNOPSIS

THIS PAGE

WAS INTENTIONALLY

LEFT BLANK

FRACTURE TOUGHNESS SYNOPSIS

According to Brown and Strawley, many well-engineered parts fail in "brittle fracture" at loads far below the stresses for which they were designed. J. H. Faupel describes BRITTLE FRACTURE as failure resulting from local plastic flow yielding without any general deformation of the material. Fracture originates at a crack or crack-like flaw. Fracture occurs at a stress well below the yield strength by crack growth (propagation). This tendency cannot be detected by conventional tensile or impact tests.

FRACTURE TOUGHNESS is the ability of a material to resist fracture in the presence of small local defects. As used in what can be called the "field of linear fracture mechanics," it is the ability to resist brittle fracture under various loads (when a crack is present) in such a manner that the crack does not grow or propagate. Since a small area ahead of the crack must yield locally so that the crack can grow, there is a local stress concentration ahead of the crack. Fracture toughness criteria are usually formulas which depend upon the strain energy or elastic stress distribution which occurs in the crack tip.

One of the easiest formulas for evaluating fracture toughness is based on the elastic stress distribution or "stress intensity" in the area ahead of the crack. It is Irwin's formula found in Brown and Strawley's article.

$$K = \sigma \sqrt{\pi \alpha} \ ,$$

where

σ = Applied stress (psi),

α = Crack length (in.),

K = STRESS INTENSITY FACTOR, (psi $\sqrt{\text{in.}}$); and

$\pi = 3.142$.

K represents the complete elastic strain field ahead of the crack. When a part is subjected to progressive tensile tearing (Figure A-1), K is replaced by K_I. A thick test specimen undergoes plane strain.

PLANE STRAIN occurs when a part cannot strain in a direction normal to the axis of an applied load, such as by contraction and/or necking in a tensile test. A triaxial tensile load with all loads of the same magnitude is an ideal example. A more practical laboratory example is a tensile test on a notched specimen thick enough so that shear failure cannot occur.

Both K and K_I are based on the assumption that the material fails by normal tensile separation rather than sliding (shear, slip).

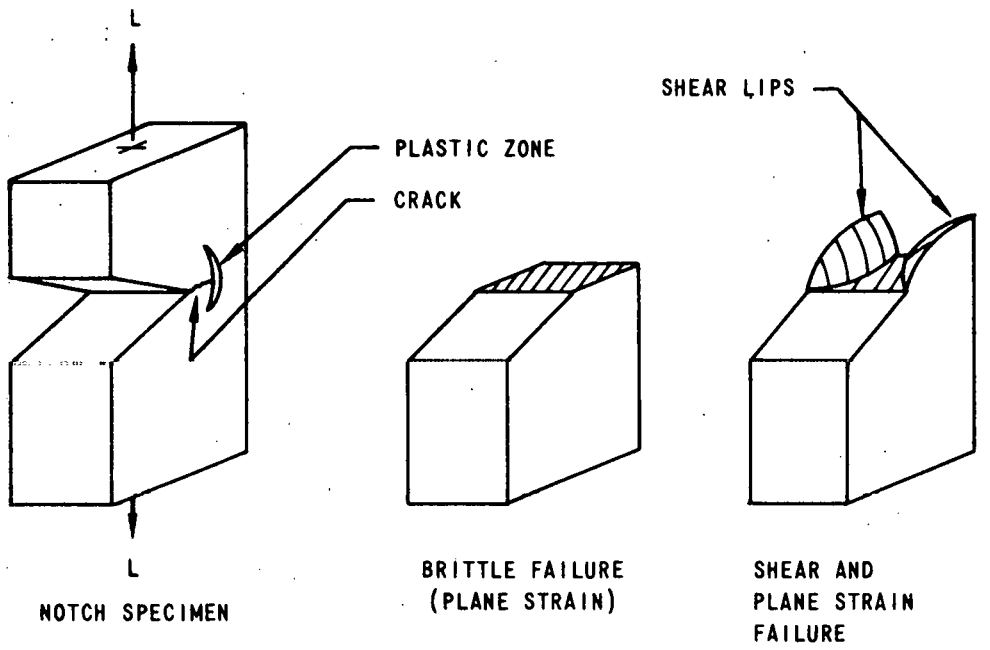

Figure A-1. Types of Tensile Cleavage Failure

Fracture in plane strain occurs when K_I reaches a critical value, K_{Ic}. This important factor is called the PLANE STRAIN FRACTURE TOUGHNESS (K_{Ic}). Ideally, K_{Ic} is independent of loading conditions and is, according to S. R. Swanson, a material constant similar to yield strength which is a constant which measures resistance to plastic flow. K_{Ic} is a stress concentration factor for a void in a material and is sensitive to temperature and processing.

When one is designing and:

$K_{Ic} = \sigma \sqrt{\pi \alpha}$

σ = The design stress, then:

α = CRITICAL CRACK LENGTH at which a stress-crack will propagate to failure (in.).

It is this crack length (α) which will be used as a criterion on polycarbonate stress-cracks.

This formula can also be used to predict if an existing crack in a service part is safe or will cause failure. If plane strain is obtained in a fracture toughness notched tensile test, the load-deflection curve will appear as in Figure A-2 below. If plane strain is not obtained because of insufficient thickness, for example, it will appear as in Figure A-3. The shape of the curve in Figure A-3 results from excessive deflection allowed by shear and slip.

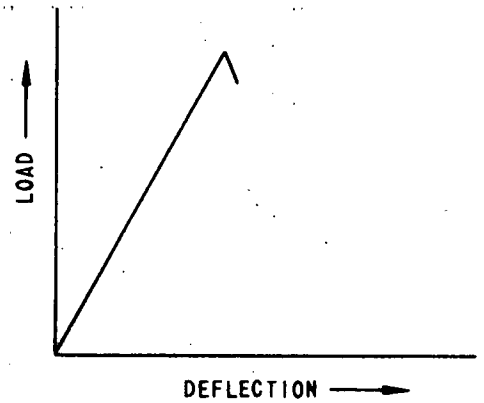

Figure A-2. Plane Strain Fracture

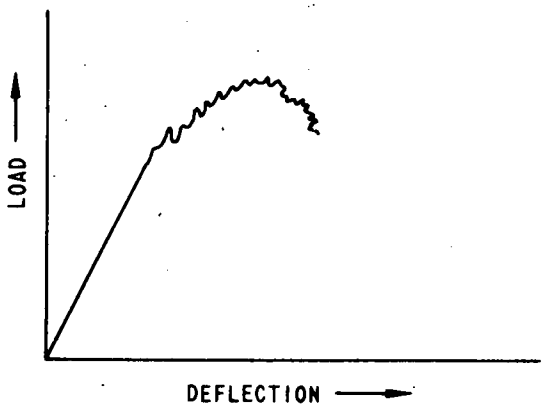

Figure A-3. Shear and Plane Strain Fracture

Since K_{Ic} can depend on geometry (shape) of the specimen, unless the plastic flow zone ahead of the crack is kept small a PLASTIC COMPLIANCE FACTOR is required in the formula for K_{Ic}.[40] This factor adjusts K_{Ic} based on the size of the plastic flow zone and gives a more accurate prediction of critical crack size. The plastic flow zone can be measured in testing.

A double edge notch specimen was used for first tests which were based on BOWIE'S FORMULA (found in Brown and Strawley, pp 10 and 11):

$$K_I = K_{Ic} = \frac{P\sqrt{\alpha}}{BW}\left[1.98 + 0.36\frac{2\alpha}{W} - 2.12\left(\frac{2\alpha}{W}\right)^2 + 3.42\left(\frac{2\alpha}{W}\right)^3\right]$$

where

B = Thickness of specimen (in.),

W = Width (in.),

P = Load (lb), and

α = Crack length: notch depth, in this case (in.).

If fracture toughness becomes significant for a material, the data will be presented in the manner shown below so that it can be used easily by the designer and systems engineer. Hence, knowing K_{Ic} (Figure A-4) and the yield strength of a given material, an engineer can evaluate such items as the sharpest notches allowed in a design, the maximum allowable residual stresses, the surface finish required, the smallest allowable holes, and the remaining service life if a crack exists. The systems engineer can set maximum allowable flaws, inclusions, and crack sizes for parts in service.

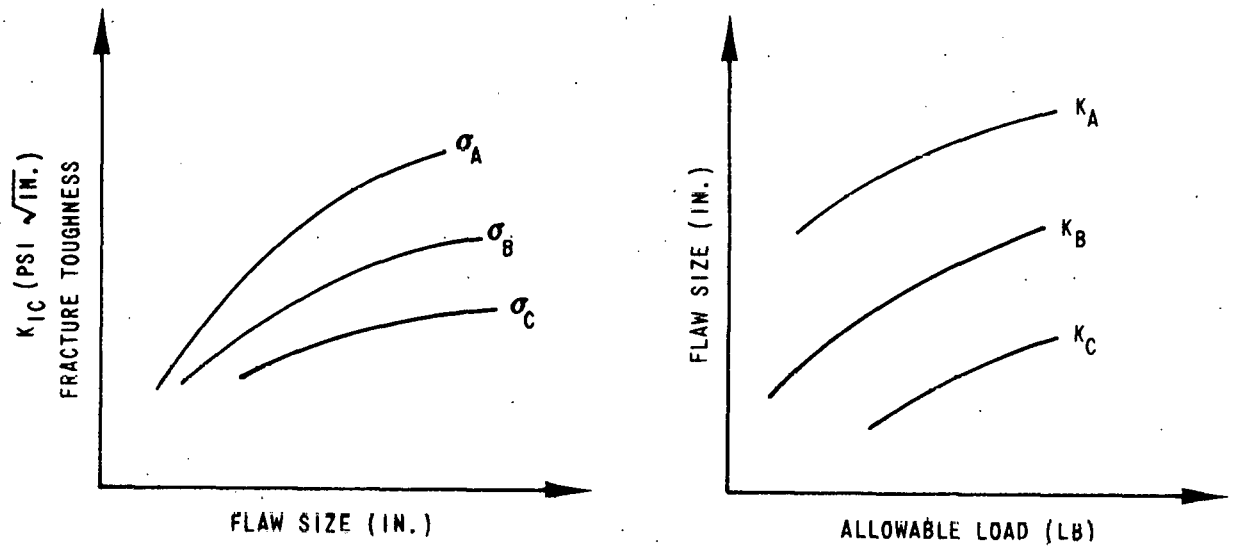

Figure A-4. Useful Parameters for K_{Ic}

Appendix B

FRACTURE TOUGHNESS COMPUTER PROGRAM FOR INTERACTION OF SPECIMEN NOTCH VARIABLES

THIS PAGE

WAS INTENTIONALLY

LEFT BLANK

Appendix B

FRACTURE TOUGHNESS COMPUTER PROGRAM FOR INTERACTION OF SPECIMEN NOTCH VARIABLES

PROGRAM DESCRIPTION

The fracture toughness program, written in Fortran IV computer language for use on an IBM 360 computer, performs a factorial analysis for an experiment with four notch factors at two levels shown below.

Symbol	Variable	Level	
A	Width	Low	High
B	Thickness	Low	High
C	Depth	Low	High
D	Radius	Low	High

Its purpose is to establish the parameters which contribute significantly to notch sensitivity (fracture toughness) and thereby affect the plastic flow zone. Significance is determined at the 90 and 95 percent level of confidence.

The program calculates fracture toughness (K_{Ic}) using Bowie's equation from ASTM-STP-410, fracture toughness (KJ) corrected for plastic compliance using Irwin's factor, gross stress (σ_1) based on specimen unnotched cross-sectional area, and net stress (σ_2) based on minimum cross-sectional area at the notch. It also makes calculations for different specimen configurations yielding values for two specimens at each configuration.

$$f = 0.1\left(\frac{K_I}{\sigma_{y.s.}}\right)^2$$

where

f = plastic compliance factor (in.),

K_I = Irwin's fracture toughness stress intensity factor (psi $\sqrt{\text{in.}}$), and

$\sigma_{y.s.}$ = yield strength (psi).

The "Yates" method of analysis for estimating the main effects and interactions for two-level factorials was used. This method is found in the U. S. Department of Commerce Handbook 9134. Only the last column of the Yates sequence is printed out, and labeled SUM + DIFFS (Tables B-1, B-2, B-3). The numerical values in this column are the indicators of significance.

These values (g) are compared to a constant (W_f) calculated for each of the 90 and 95-percent confidence levels based on a "Student t" distribution. If the (g) value is larger than the constant, the parameter involved is considered significant for that level of confidence.

Combinations of letter symbols indicate that an interaction between the corresponding variables was considered. For example, AC indicates an interaction between notch width (A) and notch depth (C). A YES in the 95 percent confidence column (Table B-3) indicates an interaction. A NO indicates no interaction, and a MABY indicates that the value compared to the constant (W_f) for that level of confidence is within 25 percent of (W_f). This means that a lower level of confidence could indicate the value as significant.

PROGRAM OUTLINE

The inputs, formulas, outputs, and variables are listed and identified below.

A. Inputs

Item		Symbol	Card Number	Columns Used
1. Materials yield strength		$\sigma_{y.s.}$	1	1-5
2. Notch Depth:	minimum	a	1	6-9
	maximum	a	1	10-13
3. Thickness:	minimum	b	1	14-17
	maximum	b	1	18-21
4. Width:	minimum	W	1	22-25
	maximum	W	1	25-29
5. Ultimate load data		P	2-33	5 per data point
Two sets of 16 data points each.				

B. Equations Used

1. Fracture toughness:[35]

$$K_I = \frac{YPa^{1/2}}{bW}$$

$$Y = 1.98 + 0.36\left(\frac{2a}{W}\right) - 2.12\left(\frac{2a}{W}\right)^2 + 3.42\left(\frac{2a}{W}\right)^3 \qquad (1)$$

P = Fracture load (lb)

a = Crack length: notch depth (in.)

W = Unnotched specimen width (in.)

b = Thickness (in.)

K_I = Fracture toughness: Opening mode (psi $\sqrt{\text{in.}}$)

2. Standard deviation:

$$\sigma X = \sqrt{\left[\sum_{i=1}^{n} X_1^2\right] - \overline{X}^2} \qquad (2)$$

σX = Standard deviation

$\overline{X}$ = Mean value of "KIAVG"

X_i = Individual values of "KIAVG"

n = Number of values for one set = 16

This formula is not printed out. A write statement could be used to do so.

3. Gross section stress:

$$\sigma_1 = \frac{P}{bW} \qquad (3)$$

σ_1 = Gross stress on unnotched section (psi)

P = Fracture load (lb)

W = Specimen Width (in.)

b = Specimen thickness (in.)

4. Net section stress:

$$\sigma_2 = \frac{P}{(W-2a)b} \tag{4}$$

σ_2 = Net stress on notched cross-section (psi)

P = Fracture load (lb)

W = Specimen thickness (in.)

b = Specimen width (in.)

a = Crack length: notch depth (in.)

5. Fracture toughness corrected for plastic flow from Equation 1:

$$K_J = \frac{YPa_o^{1/2}}{bW} \tag{5}$$

where K_J and a_o have replaced K_I and a, respectively.

From p.4 of reference in Equation 1.

$$a_o = a + \frac{1}{3\pi}\left(\frac{K_I}{\sigma_{y.s.}}\right)^2$$

$$a_o = a + 0.1\left(\frac{K_I}{\sigma_{y.s.}}\right)^2, \text{ approximately}$$

Y = Constant

K_J = K_I corrected for plastic flow (psi $\sqrt{\text{in.}}$)

a_o = Crack length corrected for plastic flow (in.)

a = Crack length (in.)

K_I = Fracture toughness (psi $\sqrt{\text{in.}}$)

$\sigma_{y.s.}$ = Material yield strength (psi)

6. Standard deviation:[36]

$$\sigma_{std.} = \sqrt{\frac{g^2_{ABC} + g^2_{ABD} + g^2_{ACD} + g^2_{BCD} + g^2_{ABCD}}{2^{n_V}}} \quad (6)$$

$\sigma_{std.}$ = Standard deviation neglecting third order effects

V = Degrees of freedom

V = 5

N = V-1

g = Respective specimen values

7. Constant of comparison for various levels of confidence:[37]

$$W_f = (2^n)^{1/2} t_f \sigma_{std} \quad (7)$$

σ_{std} = Standard deviation

n = V-1 from Equation 6

t_f = t distribution percentiles[38]

W_F = Constant for 90 and 95 percent levels of confidence

C. Outputs

Table 1

Item Description	Table Symbols
1. Sample identification in matrix experimental form	SAMPL
Width-max	A
Thickness-max	B
Notch depth-max	C
Notch tip radius-max	D
(If the letter symbol does not appear, minimum values are used.)	

2. Input values, P, Set 1	Load 1
3. Input values, P, Set 2	Load 2
4. Fracture toughness (K_I) from Equation 1	
Set 1	KI(1)
Set 2	KI(2)
5. Average value of KI(1) and KI(2)	KIAVG
6. The absolute value of the difference between (KI(1) and KI(2)	DIFF
7. The average of the DIFF column	AVERAGE DIFFERENCE
8. The average of the KIAVG column	MEAN VALUE OF KIAVG
9. The σ_X value for the KIAVG values calculated from Equation 2	STANDARD DEVIATION

Table 2

Item Description	Table Symbols
1. Sample identification-same as Table 1	SAMPL
2. Parameter relating notch depth to notch width (= 2a/W)	2A O/W
3. Values of the constant Y in Equation 2	Y*
4. Gross stress (σ_1) for Equation 4	
Set 1	S1(1)
Set 2	S1(2)
5. Net stress (σ_2) for Equation 4	
Set 1	S2(1)
Set 2	S2(2)

6. Fracture toughness (KJ) for Equation 5

Set 1	KJ(1)
Set 2	KJ(2)

7. Fracture toughness (KI) for Equation 1

Set 1	KI(1)
Set 2	KI(2)

Table 3

Item Description	Table Symbols
1. Sample identification - same as Table 1	SAMPL
2. Average value of KI(1) and KI(2)	KIAVG
3. The value of each sample for g in "Experimental Statistics	SUM + DIFFS
4. The "g" value obtained in Number 3 divided by eight	SUM + D OVER 8
5. Decision for a 95 percent confidence level If SUMS + DIFFS > W95 percent, print: YES. If 0.75 W95 percent < SUMS + DIFFS > W95 percent, print: MABY. If SUMS + DIFFS < 0.75 W95 percent, print: NO.	95% CONFID
6. Decision for a 90 percent confidence level (Same selection process is used as described in e)	90% CONFID
7. Values of the standard deviation (σ_X) as calculated by Equation 6	STANDARD DEVIATION
The constant W_f from Equation 7 for confidence level of 95 percent	OMEGA (95%)CONF
The constant W_f from Equation 7 for 90 percent confidence level	OMEGA (90%)CONF

COMPUTER PROGRAM FOR STATISTICAL ANALYSIS OF NOTCH DESIGN FACTORS

```
FORTRAN IV G LEVEL  18              MAIN          DATE=71012        17/10/52

          C   FRACTURE TOUGHNESS STATISTICAL SIGNIFICANCE MATRIX TEST
0001          Dimension CONS(6),AW(16),Y$(16),AH(16),TMAT(7,16),FKI(2,16),S1(16)
0002          Dimension AKI(16),ST1(2,16),ST2(2,16),S2(16),AN(16),SKI(2,16)
0003          Dimension X(16),AJK(2,16),AS(16),AP(16),Z(3),P(2,16),DKI(16)
0004          Data X(1)/' (1)'/,X(2)/' A '/,X(3)/' B '/,X(4)/' AB '/
0005          Data X(5)/' C '/,X(6)/' AC '/,X(7)/' BC '/,X(8)/' ABC'/
0006          Data X(9)/' D '/,X(10)/' AD '/,X(11)/' BD '/,X(12)/' ABD'/
0007          Data X(13)/' CD '/,X(14)/' ACD'/,X(15)/' BCD'/,X(16)/'ABCD'/
0008          Data Z(1)/' YES'/,Z(2)/' NO '/,Z(3)/'MABY'/
0009          Read(1,55) SYS,(CONS(I),I=1,6)
0010    55    Format (F5.0,6F4.3)
0011          DO 10 I=1,2
0012          DO 10 J=1,16
0013    10    Read(1,66) P(I,J)
0014    66    Format (F5.0)
0015          DO 20 IC=1,2
0016          L=0
0017          DO 20 M=1,2
0018          DO 20 I=1,2
0019          A=CONS(I)
0020          DO 20 J=3,4
0021          B=CONS(J)
0022          DO 20 K=5,6
0023          C=CONS(K)
0024          L=L+1
0025          AP(L)=2*A/C
0026          AS(L)=B*C
0027          AW(L)=2*A/C
0028          ST2(IC,L)=P(IC,L)/((C-2.*A)*B
0029          ST1(IC,L)=P(IC,L)/AS(L)
0030          T=AW(L)
0031          Y$(L)=1.98+.36*T-2.12*T**2+3.42*T**3
0032    20    AH(L)=Y$(L)*SQRT(A)/AS(L)
0033          DO 30 I=1,2
0034          DO 30 J=1,16
0035    30    FKI(I,J)=P(I,J)*AH(J)
0036          DO 40 J=1,16
0037          AA=FKI(1,J)
0038          BB=FKI(2,J)
0039          DKI(J)=ABS(AA-BB)
0040          AKI(J)=(AA+BB)/2.
0041          SI(J)=(ST1(1,J)+ST1(2,J))/2.
0042    40    S2(J)=(ST2(1,J)+ST2(2,J))/2.
0043          SUMS=0.
0044          SUMA=0.
0045          SUMD=0.
0046          DO 50 I=1,16
0047          SUMS=SUMS+AKI(I)**2
0048          SUMD=SUMD+DKI(I)
```

```
0049     50    SUMA=SUMA+AKI(I)
0050           SD=SUMD/16.
0051           SA=SUMA/16.
0052           SX=SUMS/16.-SA**2
0053           SX=SQRT(SX)
0054           DO 60 M=1,2
0055           L=0
0056           DO 60 I=1,2
0057           DO 60 J=1,2
0058           A=CONS(J)
0059           DO 60 K=1,4
0060           L=L+1
0061           AN(L)=A+FKI(M,L)**2/(SYS**2*3.*3.14159)
0062     60    AJK(M,L)=Y$(L)*P(M,L)*SQRT(AN(L))/AS(L)
0063           DO 65 I=1,16
0064     65    TMAT(1,I)=AKI(I)
0065           DO 70 I=2,5
0066           K=I-1
0067           DO 70 J=1,15,2
0068           L=J/2+1
0069           M=L+8
0070           TMAT(I,L)=TMAT(K,J)+TMAT(K,J+1)
0071     70    TMAT(I,M)=TMAT(K,J+1)-TMAT(K,J)
0072           DO 68 I=1,16
0073     68    TMAT(6,I)=TMAT(5,I)**2
0074           SG2=TMAT(6,8)+TMAT(6,12)+TMAT(6,14)+TMAT(6,15)+TMAT(6,16)
0075           SG=SG2/80.
0076           SG=SQRT(SG)
0077           W95=4.*2.571*SG
0078           W90=4.*2.015*SG
0079           DO 80 I=1,16
0080     80    TMAT(7,I)=TMAT(5,I)/8.
0081           Write(3,800)
0082     800   Format(1H1)
0083           Write(3,100)
0084     100   Format(2X,'SAMPL',2X,'LOAD 1',4X,'KI(1)',3X,'LOAD 2',4X,'KI(2)',4X
               1,'KIAVG',4X,'DIFF.'/)
0085           DO 200 I=I,16
0086     200   Write(3,110) X(I),P(1,I),FKI(1,I),P(2,I),FKI(2,I),AKI(I),DKI(I)
0087     110   Format(/2X,1A4,6(4X,F5.0))
0088           Write(3,120) SD,SA,SX
0089     120   Format(///3X,'AVERAGE DIFFERENCE = ',F5.0,//3X,'MEAN VALUE OF KIAV
               1G = ',F5.0,//3X,'STANDARD DEVIATION = ',F5.0)
0090           Write(3,800)
0091           Write(3,130)
0092     130   Format(2X,'SAMPL',3X,'2A0/W',5X,'Y*',9X,'S1(1)',4X,'S2(1)'
               1,4X,'KJ(1)',4X,'KI(1)',7X,'S1(2)',4X,'S2(2)',4X,'KJ(2)'
               1,4X,'KI(2)',/)
0093           DO 210 J=1,16
0094     210   Write(3,140) X(J),AP(J),Y$(J),ST1(1,J),ST2(1,J),AJK(1,J),FKI(1,J),
               1ST1(2,J),ST2(2,J),AJK(2,J),FKI(2,J)
0095     140   Format(/2X,1A4,4X,F4.3,5X,F4.2,1X,2(7X,F6.0,3X,F6.0,3X,F5.
               10,4X,F5.0))
0096           Write(3,800)
```

```
FORTRAN IV G LEVEL  18              MAIN        DATE = 71012      17/10/52

0097          W75=W95*.75
0098          W70=W90*.75
0099          Write(3,150)
0100     150  Format(2X,'SAMPL',3X,'KIAVG',4X,"SUMS+',5X,'SUM+D,6X,'95%',6X'90%
             1',/19X,'DIFFS',5X,'OVER8',4X,"CONFID',3X,'CONFID',///)
0101          DO 230 I=1,16
0102          R=ABS(TMAT(5,I))
0103          L=1
0104          M=1
0105          IF(R.GE.W95) GO TO 230
0106          L=3
0107          IF(R.GE.W75) GO TO 220
0108          L=2
0109     220  IF(R.GE.W90) GO TO 230
0110          M=3
0111          IF(R.GE.W70) GO TO 230
0112          M=2
0113     230  Write(3,160) X(I),AKI(I),TMAT(5,I),TMAT(7,I),Z(L),Z(M)
0114     160  Format(2X,1A4,4X,F5.0,4X,F6.0,4X,F5.0,5X,1A4,5X,1A4,/)
0115          Write(3,170) SG,W95,W90
0116     170  Format(///3X,'STANDARD DEVIATION = ',F8.3,//3X,'OMEGA (95% CONF)
             1= ',F5.0,///3X,'OMEGA (90% CONF) = ',F5.0)
0117          Write(3,800)
0118          STOP
0119          END
```

Table B-1. Sample Printout - I

SAMPLE	LOAD 1 (lb)	KI(1) (psi $\sqrt{in.}$)	LOAD 2 (lb)	KI(2) (psi $\sqrt{in.}$)	KIAVG (psi $\sqrt{in.}$)	DIFF (psi $\sqrt{in.}$)
(1)	482	2762	535	3066	2914	304
A	1160	3322	1230	3522	3422	200
B	1140	3367	980	2894	3131	473
AB	2400	3542	2025	2988	3265	553
C	230	2457	233	2489	2473	32
AC	900	3671	1040	4242	3957	571
BC	430	2367	485	2670	2518	303
ABC	1640	3447	1620	3405	3426	42
D	525	3009	585	3353	3181	344
AD	1360	3894	1250	3579	3737	315
BD	1030	3042	1075	3175	3108	133
ABD	2250	3320	2326	3431	3376	111
CD	180	1923	227	2425	2174	502

Table B-1 Continued. Sample Printout - I

SAMPLE	LOAD I (lb)	KI(1) (psi $\sqrt{in.}$)	LOAD 2 (lb)	KI (2) (psi $\sqrt{in.}$)	KIAVG (psi $\sqrt{in.}$)	DIFF (psi $\sqrt{in.}$)
ACD	750	3059	780	3182	3120	122
BCD	360	1982	380	2092	2037	110
ABCD	1710	3595	1710	3595	3595	0

Average difference = 257 psi $\sqrt{in.}$

Mean value of KIAVG = 3090 psi $\sqrt{in.}$

Standard deviation = 528 psi $\sqrt{in.}$

Table B-2. Sample Printout-II

SAMPLE	2 AC/W (in.)	Y*	S1(1) (psi)	S2(1) (psi)	KJ(1) (psi $\sqrt{in.}$)	KI(1) (psi $\sqrt{in.}$)	S1(2) (psi)	S2(2) (psi)	KJ(2) (psi $\sqrt{in.}$)	KI(2) (psi $\sqrt{in.}$)
(1)	0.393	2.00	5073	8352	2446	2762	5631	9271	2715	3066
A	0.197	1.99	6121	7621	2951	3322	6491	8081	3130	3522
B	0.393	2.00	6184	10180	2982	3367	5316	8751	2563	2894
AB	0.197	1.99	6527	8126	3147	3542	5507	6856	2655	2988
C	0.790	2.63	2421	11553	1656	2457	2453	11704	1678	2489
AC	0.396	2.00	4749	7867	3249	3671	5488	9090	3755	4242
BC	0.790	2.63	2332	11131	1596	2367	2631	12555	1800	2670
ABC	0.396	2.00	4460	7387	3051	3447	4405	7297	3014	3405
D	0.393	2.00	5526	9098	2664	3009	6158	10137	2969	3353
AD	0.197	1.99	7177	8935	3460	3894	6596	8212	3180	3579
BD	0.393	2.00	5587	9198	2694	3042	5831	9600	2812	3175
ABD	0.197	1.99	6119	7618	2950	3320	6323	7872	3049	3431
CD	0.790	2.63	1895	9042	1296	1923	2389	11402	1635	2425
ACD	0.396	2.00	3958	6555	2708	3059	4116	6818	2816	3182
BCD	0.790	2.63	1953	9319	1336	1982	2061	9837	1410	2092
ABCD	0.396	2.00	4650	7702	3182	3595	4650	7702	3182	3595

Table B-3. Sample Printout - III

SAMPLE	KIAVG (psi $\sqrt{in.}$)	SUMS + DIFFS (psi $\sqrt{in.}$)	SUM + D OVER 8 (psi $\sqrt{in.}$)	95% CONFID	95% CONFID
(1)	2914	49433	6179	YES	YES
A	3422	6362	795	YES	YES
B	3131	-522	-65	NO	NO
AB	3265	-627	-78	NO	NO
C	2473	-2833	-354	YES	YES
AC	3957	3131	429	YES	YES
BC	2518	227	28	NO	NO
ABC	3426	698	87	NO	NO
D	3181	-779	-97	NO	NO
AD	3737	294	37	NO	NO
BD	3108	329	41	NO	NO
ABD	3376	1271	159	NO	NO
CD	2174	-2119	-265	MABY	YES
ACD	3120	-69	-9	NO	NO
BCD	2037	1315	164	NO	NO
ABCD	3595	1103	138	NO	NO

Standard deviation = 251.294 psi $\sqrt{in.}$

Omega (95 percent conf) = 2584 psi $\sqrt{in.}$

Omega (90 percent conf) = 2025 psi $\sqrt{in.}$

REFERENCES

[1] F. W. LaMar, "Stress-Cracking of Polycarbonates," Final Report, PDO 6984695 Bendix Kansas City (August 20, 1970).

[2] H. B. Park, and D. R. Uhlman, "Recovery of Deformed Polymers - I: Retraction of Cold Drawn Polycarbonate, Polyethylene and Polypropylene," Journal of Applied Physics, Volume 41, Number 7 (June, 1970), p. 913.

[3] Bernard Rosen (ed.), Fracture Processes in Polymeric Solids: Phenomena and Theory, Interscience Publishers (New York, 1964), pp. 338, 339.

[4] Rosen, pp. 226, 228.

[5] Rosen, p. 336.

[6] Rosen, pp. 157, 161.

[7] E. T. White, B. M. Murphy and R. N. Howard, "The Effect of Orientation on the Internal Crazing of Polystyrene," Journal of Polymer Science, Part B, Volume 7 (1969), pp. 157, 161.

[8] LaMar, p. 18.

[9] Lexan-Polycarbonate Resins Design Data, General Electric Corporation Publication, Section B, Pittsfield, Mass. (July, 1966), p. 21.

[10] Injection-Molding Merlon Polycarbonate, Mobay Chemical Company Publication, Pittsburgh, p. 4.

[11] David C. Card, "Review of Fracture Theories," Strain Gage Readings, Volume 6, Number 1, (April-May, 1963), p. 14.

[12] "Fracture Toughness Testing and Its Applications," ASTM-STP-381, Symposium (June 21-26, 1964), p. 381.

[13] W. Brown, Jr., and J. Strawley, "Plane Strain Crack Toughness Testing of High Strength Metallic Materials", ASTM-STP-410 (1966), pp. 10, 11.

[14]G. R. Sippel, "Processing Effects Fracture Toughness," Metal Progress, (November, 1957).

[15]Brown, p. 61.

[16]Brown, p. 5.

[17]"Fracture Toughness Testing and Its Application", p. 14.

[18]Brown, p. 3.

[19]A. S. Tetelman, and A. J. McEvily, Fracture Toughness of Structural Materials, John Wiley (New York, 1967), p. 58.

[20]Rosen, 1. 231.

[21]Tetelman, p. 81.

[22]Tetelman, p. 620.

[23]Tetelman, pp. 621, 622.

[24]Rosen, p. 331.

[25]Tetelman, pp. 619, 256.

[26]"Fracture Toughness Testing", p. 212.

[27]Brown, pp. 15, 16.

[28]"Fracture Toughness Testing", p. 240.

[29]Brown, pp. 8, 9, 10.

[30]Rosen, p. 203.

[31]H. W. Hayden, W. G. Moffatt, and J. Wulff, "The Structure and Properties of Material," Mechanical Behavior, Volume 3, John Wiley (1965), p. 616.

[32]Rosen, pp. 201-209, 287.

[33]Tetelman, pp. 609, 621.

[34]M. C. Natrella, "Experimental Statistics," U. S. Department of Commerce, NBS, Handbook 91, pp. 12-3 through 12-8.

[35]Brown, p. 10.

[36]Natrella, p. 12-8.

[37]Natrella, p. 12-9.

[38]Natrella, p. T-5.

[39]Natrella, p. 12-8.

[40]Brown, pp. 16, 122, 123.

THIS PAGE

WAS INTENTIONALLY

LEFT BLANK

BIBLIOGRAPHY

Abbatiello, A. A., Derby, R. W., King, T. A. "Producing Epoxy-Model Pressure Vessels for Fracture Tests," Experimental Mechanics, Volume 2, Number 1, (January, 1971).

Baer, Eric. Engineering Design for Plastics. New York: Reinhold Publishing Corporation, 1964.

Barnett, R. L., Costello, J. F., Herman, P. C. "The Odds Against Fracture," Machine Design, Volume 38, Number 27, (November 10, 1966).

Bartenev, G. M., Zuyev, Yu S. Strength and Failure of Visco-Elastic Materials. Elmsford, New York: Pergamon Press, 1968.

Berry, W. E. "Stress Corrosion Cracking-A Nontechnical Introduction to the Problem," Defense Metals Information Center Report 144, Battelle Memorial Institute, Columbus, Ohio, (January 6, 1961).

Brinson, H. F. "The Ductile Fracture of Polycarbonate," Experimental Mechanics, Volume 10, Number 2, (February, 1970).

Brittain, J. O. "Modern Applications of the Theories of Elasticity and Plasticity to Metals," Symposium on Analytical Methods in the Study of Stress Strain Behavior, Boston, Massachusetts, (October 28, 1960).

Brown, W., Strawley, J. ASTM Special Technical Publication Number 410. Philadelphia: American Society for Testing and Materials, 1966.

Calcote, L. R., Bowman, C. E. "Experimental Determination of the Elastic-Plastic Boundary," Experimental Machanics, Volume 5, Number 8, (August, 1965).

Campbell, J. E. "Mechanical Properties of Metals," DMIC Review of Recent Developments, Defense Metals Information Center, Battelle Memorial Institute, Columbus, Ohio, (December 11, 1968).

Campbell, J. E. "Plane-Strain Fracture-Toughness Data for Selected Metals and Alloys," DMIC Report S-28, Defense Metals Information Center, Battelle Memorial Institute, Columbus, Ohio, (June, 1969).

Christopher, W. F., Fox, D. W. Polycarbonates. New York: Reinhold Publishing Corporation, 1962.

Clark, W. G. "How Cracks Grow in Structural Steel," Metal Progress, Volume 93, Number 5, (May, 1970).

Coffin, L. F. "The Significance of Cylic-Strain Tests in the Evaluation of Metals," Symposium on Analytical Methods in the Study of Stress-Strain Behavior, Boston, Massachusetts, (October 29, 1960).

"Conducting Creep and Time-For-Rupture Tension Tests of Materials," ASTM E139-69: 1970 Annual Book of ASTM Standards, Part 31, Philadelphia: American Society for Testing and Materials, (1970).

"Conducting Time-For-Rupture Notch Tension Tests of Materials," ASTM E292-69: 1970 Annual Book of ASTM Standards, Part 31, Philadelphia: American Society for Testing and Materials (1970).

Cord, D. C. "Review of Fracturing Theories," Strain Gage Readings, Volume 6, Number 1, (April-May, 1963).

Crews, J. H. "Elastic Plastic Stress-Strain Behavior at Notch Roots in Sheet Specimens Under Constant Amplitude Loading," NASA TN, D5253, National Aeronautics and Space Agency, (June, 1969).

Crews, J. H., Hardrath, H. F. "A Study of Cyclic Stresses at a Notch Root," Experimental Mechanics, Volume 7, Number 6, (June, 1966).

Dudderar, T. D. "Applications of Holography to Fracture Mechanics," Experimental Mechanics, Volume 9, Number 6, (June, 1969).

Dudderar, T. D., O'Regan, R. "Measurement of the Strain Field Near a Crack Tip in Polymethyl-Methacrylate," Experimental Mechanics, Volume 2, Number 2, (February, 1971).

"Environmental Stress Cracking of Test I Ethylene Plastics," ASTM D1693-70: 1970 Annual Book of ASTM Standards, Part 26, Philadelphia: American Society for Testing and Materials, (1970).

Faupel, J. H. Engineering Design. New York: John Wiley and Sons, 1964.

Forrest, P. G. "The Selection of Materials for Resistance to Fatigue," Engineering Materials-Selection and Value Analysis, New York: American Observer, 1966.

Fracture Toughness Testing and Its Applications: ASTM STP381. Philadelphia: American Society for Testing and Materials, 1964.

"Fracture Testing of High Strength Sheet Materials," ASTM Committee on Fracture Testing of High Strength Sheet Materials, (February, 1960).

Freudenthal, A. M., Heller, R. A. "On Stress Interaction in Fatigue and a Cumulative Damage Rule," Journal of Aero-Space Science, (July, 1959).

Gatts, R. R. "Application of a Cumulative Damage Concept to Fatigue," Journal of Basic Engineering, (December 1961).

A General Reference Manual for Merlon Polycarbonate. Pittsburgh: Mobay Chemical Company, 1968.

Goode, R. J. "Evaluating Alloys for Failure-Safe Structures," Metal Progress, Volume 89, Number 7, (July, 1967).

Hayden, H. W., Moffatt, W. G., Wulff, J. "The Structure and Properties of Materials," Mechanical Behavior. Volume 3. New York: John Wiley, 1965.

Hofer, K. E. "Equations for Fracture Mechanics," Machine Design, Volume 40, Number 3, (February 1, 1968).

"Injection-Molding Merlon Polycarbonate," Thermoplastics Processing, 83-M7, Pittsburgh: Mobay Chemical Company.

Kling, R. E. "Fatigue in Metals-Theory, Some Related Phenomena and Effects," Design News, Volume 20, Number 20, (October, 1965).

Knauss, W. C. "Stresses Near a Crack in a Rubber Sheet," Experimental Mechanics, Volume 8, Number 4, (April, 1968).

LaMar, F. W. 'Stress Cracking of Polycarbonates," Kansas City: Bendix Test Laboratory Report, (August, 1970).

Lever, H., Rhys, L. "The Properties and Testing of Plastics Materials." 3rd Edition. London: Temple Press Books, 1968.

Lexan-Polycarbonate Resins Design Data. Section B. Pittsfield, Massachusetts: Plastics Division, General Electric Corporation.

Lexan Polycarbonate Sheet. Pittsfield, Massachusetts: Plastics Division, General Electric Corporation, 1968.

Little, R. E. "Choosing the Right Fatigue Test," Machine Design, Volume 39, Number 28, (December 7, 1967).

Little, R. E. "How to Prevent Failure," Machine Design, Part 1, Volume 39, Number 14, (June 8, 1967) and Part 2, Volume 39, Number 18, (July 8, 1967).

McClintock, F. A. "Ductile Fracture Instability in Shear," Paper Number 58-A12. New York: American Society for Mechanical Engineers, 1958.

McEachen, G. W. Fracture Toughness Testing on Hardened 420 Stainless Steel. Kansas City: Bendix Corporation, (July, 1969).

Manson, S. S. "Fatigue: A Complex Subject-Some Simple Approximations," Experimental Mechanics, Volume 6, Number 7, (July, 1965).

Marshall, C. W. "The Factors Influencing the Fracture Characteristics of High Strength Steel," DMIC Report 147, Defense Metals Information Center, Battelle Memorial Institute, Columbus, Ohio. (February 6, 1961).

Martin, D. E. "An Energy Criterion for Low Cycle Fatigue," Journal of Basic Engineering, (December 1961).

Mukherjee, B., Culver, L. E., Burns, D. J. "Growth of Part - Through and Through Thickness Fatigue Cracks in Sheet Glassy Plastics," Experimental Mechanics, Volume 10, Number 2, (February, 1969).

Noritake, C. S., Walsh, F. D., Roberts, E. C. "Polarized Light Brings Out Details of Fracture Zones," Metal Progress, Volume 93, Number 2, (February, 1971).

"Notched Bar Impact Testing of Metallic Materials," ASTM E23-66: 1970 Annual Book of ASTM Standards, Part 31, Philadelphia: American Society for Testing and Materials, (1970).

Orange, T. W. "A Semi-Empirical Fracture Analysis for Small Surface Cracks," NASA TN D-5340, National Aeronautics and Space Agency, July, 1969.

Paris, Paul C. "Testing for Very Slow Growth of Fatigue Cracks," MTS Closed-Loop, Del Research Corporation, (1969).

Park, J. B., Uhlman, D. R. "Recovery of Deformed Polymers-I. Retraction of Cold Drawn Polycarbonate, Polyethylene and Polypropylene," Journal of Applied Physics, Volume 41, Number 7, (June, 1970).

Pinner, S. H. Weathering and Degradation of Plastics . London: Columbine Press, 1966.

"Plane Strain Fracture Toughness of Metallic Materials," ASTM 399-70T: 1970 Annual Book of ASTM Standards, Part 31, Philadelphia: American Society for Testing and Materials.

Polowski, N. H., Ripling, E. J. Strength and Structure of Engineering Materials. Englewood Cliffs, New Jersey: Prentice-Hall, 1966.

Pratt, P. L., "Fracture 1969," Proceedings of the Second International Conference on Fracture. London: Chapman and Hall, Ltd., 1969.

"Repeated Flexural Stress (Fatigue) of Plastics," ASTM D671-63T: 1968 Annual Book of ASTM Standards. Philadelphia: American Society for Testing and Materials, 1968.

Rimawi, W. H., Dogan, E., "Experiments on Yielding of Tension Specimens with Notches and Holes," Experimental Mechanics, Volume 10, Number 10, (1970).

Ritchee, P. D. Physics of Plastics. London: Iliffe Books Ltd., 1965.

Roberts, E. "Elastic Crack-Edge Displacements for the Compact Tension Specimen," ASTM Bulletin (Feburary, 1969).

Robinson, E. "Brittle Materials," Machine Design, Volume 37, Number 21, (September 2, 1965).

Rosen, Bernard. Fracture Processes in Polymeric Solids - Phenomena and Theory . New York: Interscience Publishers, 1964.

Schnell, H. Chemistry and Physics of Polycarbonates. New York: Interscience Publishers, 1964.

Serenson, S. V., Schneiderovich, R. M. "Deformations and Rupture Criteria Under Low-Cycles Fatigue," Experimental Mechanics, Volume 6, Number 12, (December, 1966).

Shannon, J. L., Brown, W. F. "Progress in Fracture Mechanics," Machine Design, Volume 42, Number 6, (March 5, 1970).

Shannon, John L. "Fracture Mechanics: Reducing Theory to Practice," Machine Design, Volume 39, Number 24, (October 12, 1967).

Shannon, John L. "Fracture Mechanics: The Search for Safety in Numbers," Machine Design, Volume 39, Number 23, (September 28, 1967).

"Sharp Notch Tension Testing of High Strength Sheet Materials," ASTM E338-68: 1970 Annual Book of ASTM Standards, Part 26, Philadelphia: American Society for Testing and Materials, (1970).

Sippel, G. R. "Processing Affects Fracture Toughness," Metal Progress, Volume 90, Number 11, (November, 1967).

Solntsev, S. S. "Analysis of the Fracture of Glass from the Path of Cracks and From the Structure of Glass," (Russian Translation), UDC 620.192:655, 1/2, Zavodskaya Laboratoriya, Volume 31, Number 6, (June, 1965).

Sparboe, D. I. "Engineers' Guide to Polycarbonate Plastics," Materials Engineering, Volume 72, Number 12 (December, 1970).

Spewock, M., Ceschini, L. J. Fracture Toughness Testing of Large-Scale Specimens. Westinghouse Electric Corporation, 1970.

Steigerwald, E. A. "What You Should Know About Fracture Toughness," Metal Progress, Volume 90, Number 9, (September, 1967).

Stulen, F. B., Cummings, H. N., Schulte, W. C. "A Design Guide: Preventing Fatigue Failures - Part 6 - Biaxial Fatigue Stresses," Machine Design, Volume 29, Number 18, (July 6, 1961).

Swanson, S. R. "The Elements of Fracture Mechanics." Society for Experimental Stress Analysis, Minneapolis - St. Paul Chapter Meeting, (January 31, 1968).

Swanson, S. R. "The Elements of Fracture Mechanics," MTS Closed-Loop, MTS Systems Corporation, Minneapolis, Volume 2, Number 2.

Tetelman, A. S., McEvily, A. J. Fracture of Structural Materials. New York: John Wiley, 1967.

Thompson, R. J. Photoelastic Analysis and Model Fringe Value of Lexan Polycarbonate Resin. Pittsfield, Massachusetts: Chemical Materials Department, General Electric Corporation, 1962.

Tomasetti, T. A., Bauer, F. A. Testing of Molded Polycearbonate for Residual Molding Stresses-Solvent Stress Analysis. Pittsfield, Massachusetts: Plastics Division. General Electric Corporation, 1969.

Wendle, B. C. "Can You Use Polycarbonate?" Materials Engineering, Volume 70, Number 6, (June, 1968).

White, E. T., Murphy, B. M., Haward, R. N. "The Effect of Orientation on the Internal Crazing of Polystyrene," Journal of Polymer Science, Part B, Volume 7, (1969).

Wigley, D. A. "Fracture Toughness Testing at Cryogenic Temperatures," Cryogenics, Volume 10, Number 7, (October, 1970).